



Neoproterozoic hydrothermally altered basaltic rocks from Rajasthan, northwest India: Implications for late Precambrian tectonic evolution of the Aravalli Craton

B. Van Lente^a, L.D. Ashwal^{b,*}, M.K. Pandit^c, S.A. Bowring^d, T.H. Torsvik^{b,e,f}

^a Deswik Mining Consultants, 193 Hole-in One Road, Ruimsig, Johannesburg, 1724 South Africa

^b School of Geosciences, University of the Witwatersrand, Private Bag 3, WITS 2050, South Africa

^c Department of Geology, University of Rajasthan, Jaipur 302 004, India

^d Department of Earth, Atmospheric and Planetary Sciences, MIT, Building 54-1124, Cambridge, MA 02139, USA

^e Centre for Geodynamics, Geological Survey of Norway, Leiv Erikssons vei 39, N-7491 Trondheim, Norway

^f PGP, University of Oslo, N-0316 Oslo, Norway

ARTICLE INFO

Article history:

Received 11 April 2008

Received in revised form 22 January 2009

Accepted 22 January 2009

Keywords:

Hydrothermal alteration

Punagarh and Sindreh Groups

U–Pb geochronology

Geochemistry

Aravalli Craton

NW India

ABSTRACT

The isolated volcano-sedimentary sequences of the Punagarh and Sindreh Groups occur along the western flank of the Delhi Fold Belt in northwest India, and include mafic rocks (pillow basalts and dolerite dykes) that are dominantly olivine tholeiites with minor quartz-normative and alkali basalts. Sindreh samples appear to have higher primary TiO_2 and P_2O_5 abundances relative to those from Punagarh. Both suites of mafic rocks show variable, but profound hydrothermal alteration effects, with loss on ignition (LOI) values up to 10.3 wt.%, and extensive secondary minerals including albite, sericite, chlorite and calcite. Despite this, there is excellent preservation of magmatic textures, but there has been extensive albitization of plagioclase phenocrysts, a hallmark of hydrothermal alteration processes in oceanic crust. Supporting evidence for such hydrothermal alteration comes from correlations of LOI abundances with $\text{CaO}/\text{Na}_2\text{O}$, and evidence for U mobility is apparent on diagrams of Nb/Th vs. Nb/U. Felsic volcanic rocks (rhyolite, dacite) interlayered with the Sindreh basalts yield U–Pb zircon ages (TIMS method) between 761 ± 16 and 767 ± 3 Ma, which we interpret as representing the time of primary magmatic activity. We infer that the volcano-sedimentary rocks of the Punagarh also formed at this time, on the basis of similarities in lithology, stratigraphy, field relations and geochemistry. Intermediate granitoid rocks yield older U–Pb ages of 800 ± 2 and 873 ± 3 Ma, which we correlate with the post-Delhi Supergroup Erinpura Granites. Taken together, the features of the Punagarh and Sindreh Groups are consistent with their formation in a back-arc basin setting. Their coevality with other magmatic systems in NW India (Malani Igneous Suite), the Seychelles and Madagascar, for which a continental arc setting has also been proposed, supports the notion of an extensive convergent margin in western Rodinia at 750–770 Ma.

© 2009 Elsevier B.V. All rights reserved.

1. Introduction

The Aravalli Craton of northwestern India, exposed over 80,000 km² in the states of Rajasthan and northern Gujarat (Fig. 1), consists of a variety of Archaean to Proterozoic rocks, and is overlain by undeformed Phanerozoic sedimentary sequences (Heron, 1953; Gupta et al., 1997). Although the Craton has been reasonably well mapped, there is a paucity of precise geochronology and modern geochemical and isotopic data. Accordingly, many of the key tectonic and stratigraphic relationships are unclear, and represent issues of vigorous contention. In many cases, divergent interpreta-

tions of basement-cover relations and/or stratigraphic associations have led to conflicting tectonic models, as discussed below. In this paper we contribute to the expanding database of geological, petrologic, geochemical and chronological information for the Aravalli Craton. Specifically, we attempt to resolve the stratigraphic position of Sindreh and Punagarh Groups, two Neoproterozoic basaltic to rhyolitic sequences, and related metasedimentary rocks in the southwestern part of the Craton. We also discuss the petrogenesis of these rocks, and their significance for tectonic models of late Precambrian continental evolution.

2. Geological overview

The oldest rocks in the Aravalli Craton (Fig. 1), referred to as the Banded Gneiss Complex (BGC), consist dominantly of amphibolite to granulite grade, tonalitic to granodioritic gneisses, with

* Corresponding author. Tel.: +27 11 717 6652; fax: +27 11 717 6579.

E-mail addresses: belindavl@datamine.co.za (B. Van Lente), Lewis.Ashwal@wits.ac.za (L.D. Ashwal), mpandit_jp1@sancharnet.in (M.K. Pandit), sbowring@mit.edu (S.A. Bowring), Trond.Torsvik@ngu.no (T.H. Torsvik).

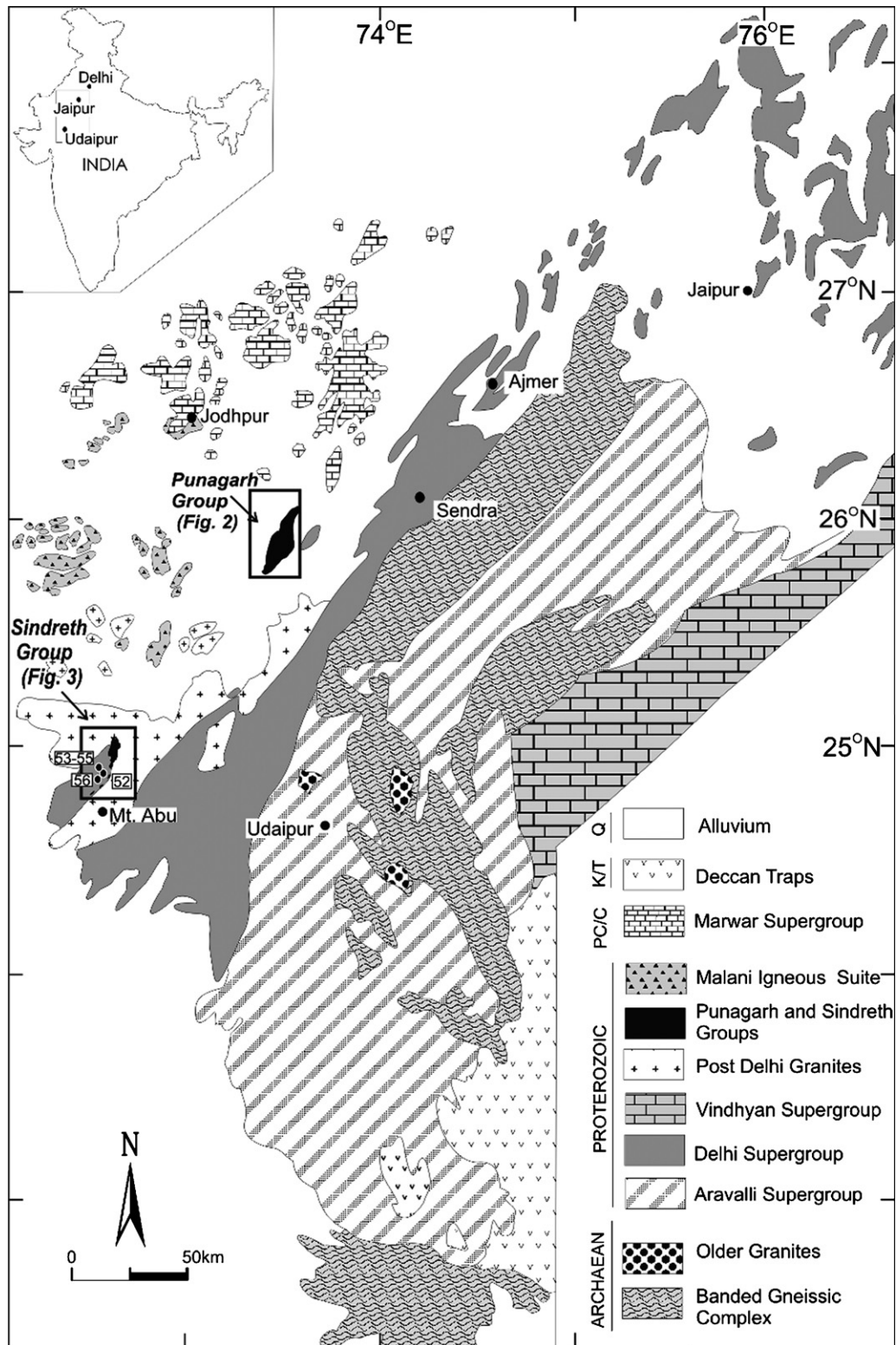


Fig. 1. Regional geological map of the Aravalli Craton, adapted from Heron (1953), Sharma (1995), Chore and Mohanty (1998), Roy and Jakhar (2002), and maps published by the Geological Survey of India. Locations of study areas (Figs. 2 and 3) are indicated.

associated lenticular masses of amphibolite (Heron, 1953), that yield ages of ~3.3 to ~2.4 Ga, using various methods (Gopalan et al., 1990; Wiedenbeck and Goswami, 1994; Wiedenbeck et al., 1996; Roy and Kröner, 1996). Two supracrustal sequences, both of which include metasedimentary and metavolcanic rocks, post-date the BGC; these are the Aravalli and the Delhi Supergroups,

of presumed Palaeoproterozoic and Meso- to Neoproterozoic ages, respectively (Gupta et al., 1997). Contact relationships within and between these supracrustal rocks are equivocal, as are their structural relationships to the BGC (e.g. Ahmad and Tarney, 1994). The Aravalli Supergroup was considered by Heron (1953) to unconformably overlie the BGC, whereas Naha and Halyburton (1974) and

Naha and Roy (1983) interpreted the boundary as a migmatization front. Likewise, the tectonized contact between the Aravalli and Delhi Supergroups has been discussed as an unconformity (Heron, 1953; Saini et al., 2006), or as a suture representing the closure of a Proterozoic ocean (Sugden et al., 1990).

The Aravalli Supergroup consists of a thick basal unit of mafic volcanics with intercalated quartzite and conglomerate, followed upward by calcareous and argillaceous sedimentary rocks (Sinha-Roy et al., 1998; Roy and Jakhar, 2002). The age and time span of Aravalli sedimentation are poorly constrained, but must have initiated later than ~2.5 Ga, based on ion microprobe U–Pb analyses of zircon from basement gneiss and granitoids in the Aravalli Craton (Wiedenbeck et al., 1996). These rocks document a complex deformational and metamorphic history, involving three major phases of folding and repeated shearing, several sets of small scale folds, crenulations and kink bands, with metamorphic grades varying from lower greenschist to upper amphibolite facies (Roy and Jakhar, 2002 and references therein). The age(s) of these events are also poorly constrained.

Rocks of the Delhi Supergroup represent the dominant geomorphic component of the Aravalli mountain range, and constitute a highly deformed, NE–SW trending linear fold belt ~800 km long between Delhi and northern Gujarat (Fig. 1). Lithologies consist mainly of clastic and chemical metasedimentary rocks that have been tightly folded into a regional synclinorium, with evidence for polyphase deformation and metamorphic grade varying from greenschist to upper amphibolite (Heron, 1953). According to Gupta et al. (1997), deposition of Delhi rocks in the southern domain successively took place in shelf margin (arenaceous–argillaceous facies – Gogunda Group), shelf interior (calcareous–argillaceous facies – Kumbhalgarh Group), geosynclinal troughs (clastic sediments of Sirohi Group) and post-orogenic successor basins (molasse sediments of the Sindreth and Punagarh Groups). Infolded with the Kumbhalgarh Group carbonate-bearing units are a series of amphibolitic mafic to ultramafic rocks that have been discussed in terms of a possible ophiolitic origin, based on their geochemical affinities to MORB and island-arc basalts (Phulad Ophiolite Suite, Volpe and Macdougall, 1990). The Sirohi Group has been described as essentially an ensemble of argillaceous rocks comprising phyllite and mica (biotite) schist with minor intercalations of quartzite and marble. The overlying, N–S trending Sindreth Group has been described to represent the post-orogenic phase of Delhi cycle, which includes a synformally folded lithopackage comprising conglomerate, quartzite, shale, phyllite and syn-sedimentational basic lava flows. The status of the Sirohi Group and younger rocks is, however, contentious.

The chronological history of Delhi Supergroup rocks is based mainly on whole-rock Rb–Sr ages of presumably intrusive granitoids (Choudhary et al., 1984), which show a geographic distribution such that an older group (~1.5–1.7 Ga, Choudhary et al., 1984; ~1.75 Ga, Biju Sekhar et al., 2003) evidently is spatially restricted to the northeastern exposures of the Delhi Supergroup, and younger groups (~1 and 0.85 Ga) occur southwest of Ajmer (Fig. 1). In current usage, the volumetrically more abundant, ~0.83 Ga granitoids are known as ‘Erinpura granites’ (Heron, 1953), whose syn- to late-tectonic nature has been linked to the terminal phases of the Delhi “orogeny” (Sharma, 1977). The spatial and temporal separation of Proterozoic granitoids has led to the suggestion that sedimentation of the Delhi Supergroup was also widely separated in space and time, with the northeastern part of the belt representing a Mesoproterozoic basin, and the southwestern exposures representing a Neoproterozoic one (Sinha-Roy, 1984; Bose, 1989). Some later workers have questioned the temporal subdivision of the Delhi Supergroup (e.g. Roy and Jakhar, 2002). There are some precise U–Pb ages available on the Sendra granitoids (Deb et al., 2001; Pandit et al., 2003), however, the geochronological informa-

tion on the Erinpura granitoids is mostly based on imprecise Rb–Sr data (Choudhary et al., 1984) and awaits precise U–Pb zircon dating, some of which is in progress.

Based on the analogy that the Delhi Supergroup rocks show a general younging towards the west, both the Punagarh and Sindreth Groups, occurring along the western margin of the Delhi Fold Belt, have been described as either the youngest units of, or as younger than the Delhi rocks (Gupta et al., 1997; Roy and Jakhar, 2002). Both of these Groups are exposed along linear trends and are seen unconformably resting over a basement of Erinpura granite and granite gneisses. The other evidence for their correlation is based on the lithological similarity (bimodal volcanism, volcanoclastic and terrigenous sedimentary rocks) and lower degree of deformation and metamorphism relative to the principal units of the Delhi Supergroup.

The youngest of the Precambrian sequences in the Aravalli Craton is referred to as the Malani Igneous Suite (MIS), which has been said to represent the world’s third largest felsic volcanic/plutonic province (Pareek, 1981; Bhushan, 2000). These Neoproterozoic rocks are variably exposed over ~51,000 km², and consist dominantly of unmetamorphosed rhyolitic and rhyodacitic volcanics (and minor basalt), with associated granitoid intrusions that clearly unconformably overlie or intrude into metasedimentary rocks of the Delhi Supergroup. Two distinct geochemical types of MIS silicic magmatic rocks have been identified, including peraluminous (Jalore type) and peralkaline (Siwana type) varieties (Eby and Kochhar, 1990). The MIS rocks are, in places, gently tilted and folded (Mukherjee, 1966), and are unconformably overlain by flat-lying evaporites and redbeds (Marwar Supergroup) of presumed Latest Neoproterozoic/Cambrian age (Pandit et al., 2001). Magmatic ages for MIS rocks, based on TIMS U–Pb zircon data range between 771 and 751 Ma (Torsvik et al., 2001a; Gregory et al., 2009), in agreement with Rb–Sr whole rock data (730 ± 10 Ma, Crawford and Compston, 1970). Palaeomagnetic work (Torsvik et al., 2001a; Gregory et al., 2009) suggests that the MIS may have been contiguous with similar ~750 Ma granitoid rocks of the Seychelles and possibly northeastern Madagascar, which collectively have been interpreted as having formed in an Andean-type arc setting (Ashwal et al., 2002).

Attempts to model the post-Delhi acid magmatic events on the basis of published geochronological data have led to an overlap of the geochronological history of the Erinpura granite with the MIS (Choudhary et al., 1984; Sivaraman and Raval, 1995; Dhar et al., 1996; Rathore et al., 1996, 1999; Torsvik et al., 2001a; Gregory et al., 2009). Published geochronological data for the Neoproterozoic magmatic events along the western flank of the South Delhi Fold Belt and farther west (including MIS) were mostly based on whole-rock Rb–Sr isochrons (or errorochrons).

3. Punagarh and Sindreth Groups: outline of the present study

Two isolated volcano-sedimentary sequences occur along the western flank of the Delhi Fold Belt (Figs. 1–3), and are designated as the Punagarh and Sindreth Groups (Chore and Mohanty, 1998). They are exposed in elongate to oval-shaped, NNE–SSW trending areas of ~150 km² (Punagarh, Fig. 2) and ~40 km² (Sindreth, Fig. 3), separated by ~110 km; the intervening regions are composed mainly of Erinpura-type granitoids (Fig. 1). Outliers of units similar to those in the Sindreth Group occur within phyllites and mica schists of the Delhi Supergroup up to 10 km southwest of the southern edge of the main Sindreth outcrop area (Fig. 3; Gupta et al., 1997). Lithologies are remarkably similar in both the Punagarh and Sindreth Groups, consisting of clastic sedimentary rocks including shale, slate, phyllite, micaceous schist, quartzite and conglomerate, with associated basaltic lavas (commonly pillowed), bedded chert, and subordinate felsic volcanic rocks and tuffs (Chore and Mohanty, 1998; Gupta et

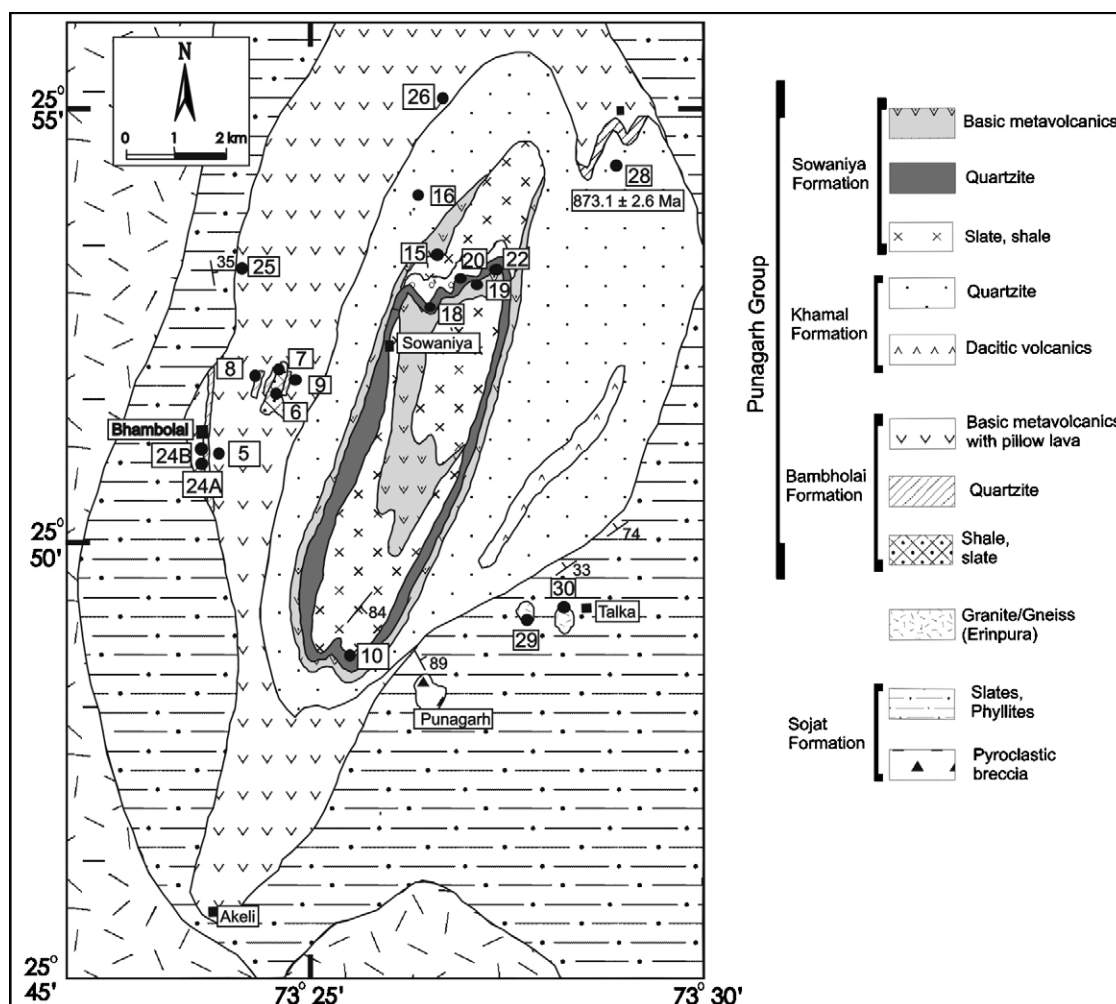


Fig. 2. Geological map of the Punagarh area, Pali District, Rajasthan, modified after Chore and Mohanty (1998).

al., 1997). These sequences are both folded into synclinal structures, although metamorphic grade is quite low (sub- to mid-greenschist).

The Punagarh Group, which unconformably overlies the sedimentary rocks of the Sojat Formation, is subdivided into three formations: the Bambholai, Khambal and Sowaniya Formations (Fig. 4). The total thickness of the Punagarh Group can be estimated at ~4500 m, but which is duplicated due to folding. The unconformable relationship is revealed by the moderately dipping (~30°) basic Punagarh flows that rest over the steeply dipping (~75°) beds of the Sojat phyllites (Chore and Mohanty, 1998). The Bambholai Formation unconformably overlies the Sojat Formation, the latter intruded by the EG. The Bambholai rocks themselves are devoid of any granitic intrusions and mainly contain pillow basalts, with interlayered beds of shale and quartzite. The Khambal Formation is in contact with the Sojat Formation only on the eastern limb of the Punagarh basin (Fig. 2). Bedded chert and vesicular and amygdaloidal volcanic rocks were deposited on top of the quartzite. The Sowaniya Formation consists of repetitive felsic and basic flows, with an upper shale horizon and quartzite resting over the volcanics of the Khambal Formation (Chore and Mohanty, 1998). Structurally, the Punagarh Group is a doubly plunging, NNE-trending asymmetric syncline produced during a first phase of deformation (F1). Fold axes trend N25°E and plunge 35–55° towards the NNE and SSW. Planar structures (S1) related to the first deformational phase trend NNE and show vertical to subvertical dips. A second phase of deformation (F2) resulted in cross-fold and rare broad warps, the latter trending N70°E. Intrusive granitoids are restricted to the Sojat For-

mation and do not crosscut the Punagarh Group rocks. The youngest intrusive activity is represented by dolerite dykes that crosscut both the Sojat Formation and the Punagarh Group.

On the basis of rock associations the Sindreth Group (thickness ~500 m) is subdivided into the Khambal and Angor Formations that are inferred to unconformably overlie the Sirohi Group (Figs. 3 and 4). The unconformable relationship is inferred by the intrusion of Erinpura granite (EG) into the Sirohi Group, whereas the Sindreth Group rocks are devoid of granitic intrusions (Chore and Mohanty, 1998). The unconformable relationship between the EG and the Khambal Formation is indicated by the basal polymictic conglomerate at the interface (Chore and Mohanty, 1998). The Angor Formation contains mainly felsic volcanic rocks and bedded chert, ash flow tuff and ignimbrite that are restricted to the N-S trending ridges and represent the basal part of the formation (Chore and Mohanty, 1998). WNW to N-S trending dolerite dykes crosscut the Sirohi and Sindreth Group rocks as well as the EG. These dykes follow the same trend as felsic dykes that have been correlated with the terminal phases of the MIS (Chore and Mohanty, 1998). Structurally, the Sindreth Group shows a simpler deformation history relative to the Punagarh Group. Chore and Mohanty (1998) report a single phase of deformation, while Roy and Jakhar (2002) found no evidence of deformation. The ensemble of bimodal volcanic and sedimentary rocks shows a general N-S trend with moderate westerly dips.

The stratigraphic position of the Punagarh and Sindreth sequences is debated. Some workers consider these rocks to rep-

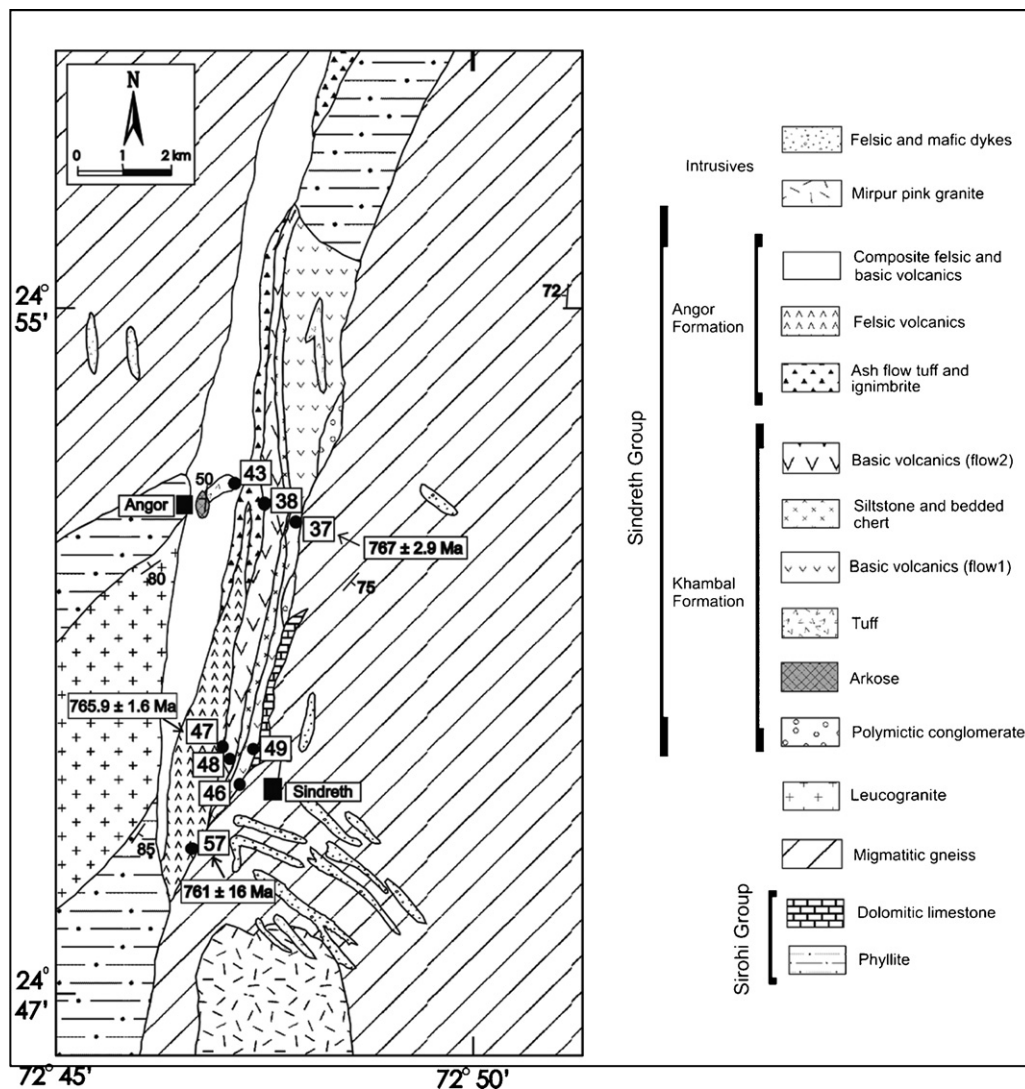


Fig. 3. Geological map of the Sindreth area, Rajasthan, modified after [Chore and Mohanty \(1998\)](#).

represent the youngest members of the Delhi Supergroup (e.g. [Singh, 1982](#); [Gupta et al., 1997](#); [Sinha-Roy et al., 1998](#)), whereas others (e.g. [Bose, 1989](#); [Roy and Sharma, 1999](#)) interpret them as precursors to MIS magmatism. Still others interpret the Punagarh and Sindreth rocks to have formed independently, in the time gap between Erinpura (~830 Ma) and Malani (750–771 Ma) magmatism (e.g. [Chore, 1990](#); [Chore and Mohanty, 1998](#)). Each of these possibilities has important consequences for the tectonic evolution of the Aravalli Craton, and can be resolved using precise geochronology. We report here U–Pb zircon data (single-crystal TIMS method) in an attempt to resolve the stratigraphic position of the Punagarh and Sindreth Groups, as well as geologic, petrologic, geochemical and isotopic data relevant to their petrogenesis and tectonic setting. Our focus is mainly on the volcanic and spatially associated intrusive rocks.

4. Analytical methods

Major element compositions were determined using a Phillips PW1480 wavelength dispersive XRF spectrometer, housed at the Univ. of Cape Town, Dept. of Geological Sciences. Fusion disks for each sample were prepared according to the methods described in [Norrish and Hutton \(1969\)](#), [Duncan et al. \(1984\)](#) and [Heinrich \(1986\)](#). All measurements were made with a dual target Mo/Sc X-ray tube at 50 kV, 50 mA. Fusion disks made up with 100% Johnson

Matthey Specpure SiO_2 were used as blanks for all elements except Si, for which mixtures of Johnson Matthey Specpure Fe_2O_3 and CaCO_3 were used.

Trace elements, including REE, were analysed by ICP-MS using standard techniques. The solutions represented 1000-fold dilutions of the original solid samples and were analysed in the ICP-MS, housed at the Univ. of Cape Town, Dept. of Geological Sciences. Mineral compositions were determined using a Camebax 355 electron microprobe with an attached Lemas Exl II EDS detector, housed at Rand Afrikaans Univ., Dept. of Geology. Natural mineral standards were used for calibration, and the operating conditions were used 15 kV, 15 nA, 50 s counting times, 10 μm beam diameter (feldspars) or 5 μm (pyroxenes, Fe–Ti oxides, glass).

Samples for U–Pb zircon age analyses were cleaned, pulverized and zircons separated using standard techniques; analyses were performed at the Massachusetts Institute of Technology, Dept. of Earth, Atmospheric and Planetary Sciences. Zircon grains were air-abraded with pyrite at 2 psi for ~15–20 h. The U and Pb concentrations and isotopic compositions were determined using a VG Sector 54 thermal ionization mass spectrometer housed at MIT. Precision and accuracy of data in [Table 3](#) are at 2σ with 95% confidence levels.

Samples for Sm–Nd isotopic analyses were dissolved in mixed HF-HNO_3 (3:1) and chemical separation was carried out by cation-

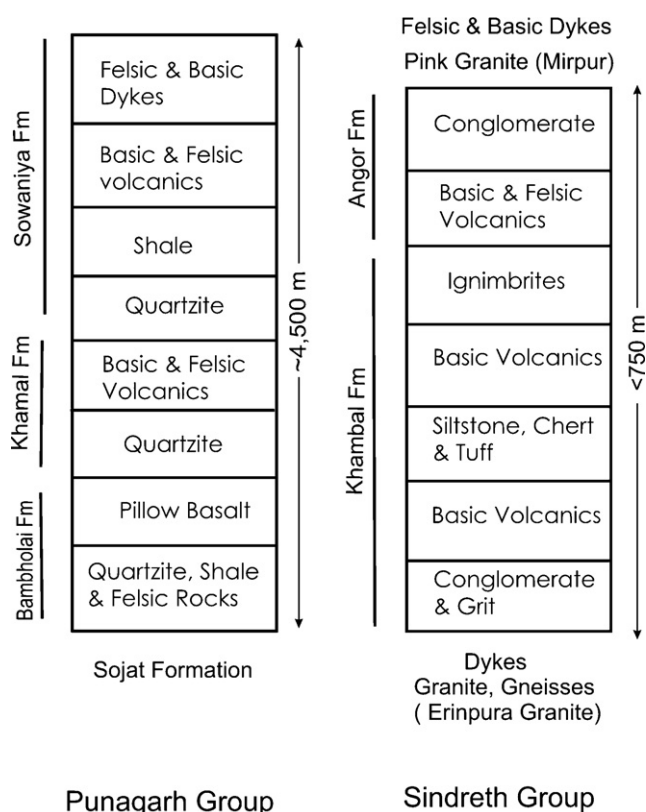


Fig. 4. Schematic stratigraphic columns of supracrustal units in the Punagarh and Sindreth Groups. Modified after [Chore and Mohanty \(1998\)](#).

exchange chromatography; procedural blanks were <1 ng. Isotopic ratios were measured on a VG Sector 54 mass spectrometer at the Massachusetts Institute of Technology.

5. Results

5.1. Lithologies, petrography and mineral chemistry

Visually estimated modes of all the rocks studied are given in [Table 1](#). The Punagarh basalts (BVL-005A, 005C, 008A to 008C, 0019, 0024A, 0024B, 0026A and 0026B) are dark grey coloured, fine-grained rocks consisting of plagioclase laths (mostly altered to albite and sericite), clinopyroxene (mostly altered to chlorite), opaques (ilmenite, magnetite, rutile and pyrite), chlorite and epidote, in a fine-grained groundmass ([Fig. 5](#)). In some specimens the groundmass consists of devitrified glass and chlorite. The Sindreth basalts (BVL-0037A, 0046A to 0046F, 0048, 0049) are black to dark green fine-grained rocks, characterised by the presence of amygdaloidal and vesicular structures ([Roy and Sharma, 1999](#)). These basalts consist of microphenocrysts (<1 mm) and some larger lath-shaped phenocrysts (~5 mm) of plagioclase (mostly altered to albite and sericite), clinopyroxene (mostly altered to chlorite), magnetite, ilmenite and rutile, and secondary quartz in a fine-grained, mostly altered and in some cases glassy, groundmass. The vesicles (size varies from ~2 mm to ~1 cm) have been filled with quartz and calcite, and minor amounts of epidote and zeolite.

Primary calcic plagioclases of both the Punagarh and Sindreth basalts have been variably altered into albite-rich compositions, such that some samples preserve primary compositions, whereas others have been partly to totally albitized ([Fig. 5](#)). Primary compositions of An_{44-67} are best preserved in samples BVL-008C, 0046B and 0046D. Others, such as BVL-008B, 0026B and 0046A, show a

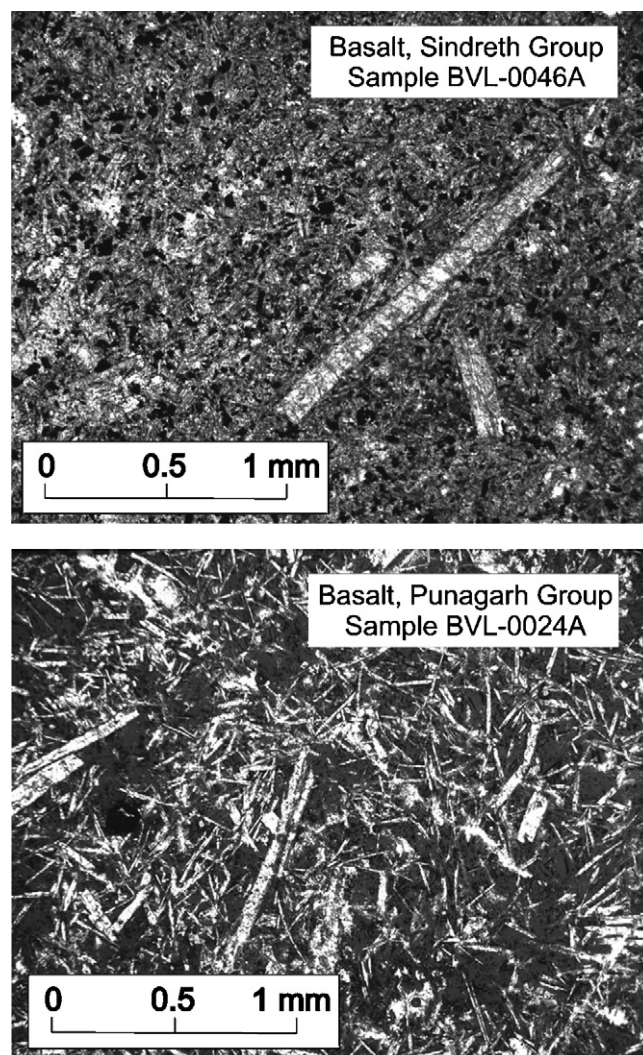


Fig. 5. Photomicrographs of typical hydrothermally altered basaltic rocks from the Sindreth and Punagarh Groups, showing well preserved magmatic texture consisting of variably sericitized plagioclase phenocrysts in a groundmass of devitrified glass, Fe–Ti oxides and chloritized clinopyroxene. Plagioclase in BVL-0024A is completely albitized ($An_{0.4-5.8}$), whereas very minor relict magmatic compositions are preserved in BVL-0046A ($An_{2.5-63.9}$).

large spectrum of compositions between primary values of An_{64} and secondary albite-rich compositions down to $An_{0.4}$. In several samples (e.g. BVL-005A, 005C, 0019, 0024A, 0024B and 0038) plagioclase has been completely albitized. It is important to note that primary magmatic textures are very well preserved in all specimens. Due to the extent of the alteration of the plagioclase phenocrysts to albite and sericite, it was not possible to determine the degree of possible primary magmatic zoning.

Clinopyroxenes in all of the studied Punagarh and Sindreth mafic samples have been extensively altered to chlorite, with only parts of some of the crystals retaining relict primary pyroxene. These pyroxenes are augite with Mg-numbers of 0.414–0.586 ([Table 1](#)). The high content of TiO_2 (avg. = 1.92 ± 1.65 wt.%, $n = 12$) in the clinopyroxenes of the basalts is typical of basic alkaline rocks. The augites are sub-calcic in composition, and no exsolution lamellae were found in any of the studied samples. Even though zoning is a relatively common feature of augites, and particularly in titanian varieties, no evidence for this could be found due to the high degree of alteration.

The pillow basalts of both the Punagarh and Sindreth Groups (BVL-005, 008, 0024 and 0038) contain devitrified glass as part of the groundmass. Analyses of these indicate high TiO_2 values

Table 1

Visually estimated modes and summary of microprobe data for Delhi Supergroup and Punagarh and Sindreth Group rocks.

Mafic rocks										
	Punagarh Group									
	BVL-005A Plagioclase-phyric basalt	BVL-005C Plagioclase-phyric basalt	BVL-007 Massive volcanic breccia	BVL-008A Plagioclase-phyric basalt	BVL-008B Plagioclase-phyric basalt	BVL-008C Plagioclase-phyric basalt	BVL-008D Plag-phyric basalt (pillow rim)	BVL-009A Altered dolerite	BVL-009B Altered dolerite	BVL-0014B Altered dolerite
Plagioclase	35	30	35	35	35	35	25	31	23	8
Clinopyroxene				30	30	28		30	15	
Fe–Ti oxides	2		5	10	10	10	7	4	4	8
Glass (devitrified)	51	44	15				58			
Sericite	5	10		2	2	2		20	30	45
Amphibole										
Chlorite	4	8	25	20	23	25	10	15	20	27
Biotite										
Calcite	3	5	18	3	tr					7
Epidote		3								
Quartz			2						8	5
Sphene										
Pyrite										
Hematite										
An content (mol%)										
Mean	5.11	6.68		5.55	20.75	60.25		44.04		
Range	0.80–16.58	2.30–15.39		0.85–24.67	4.76–59.85	50.47–65.09		24.18–68.52		
Cpx Mg# (range)				0.48–0.53	0.46–0.53	0.59–0.61		0.74–0.83		
Mafic rocks										
	Punagarh Group									
	BVL-0015 Altered dolerite	BVL-0016 Altered dolerite	BVL-0018 Altered dolerite	BVL-0019 Altered dolerite	BVL-0020 Dolerite/gabbro	BVL-0024A Plagioclase-phyric basalt	BVL-0024B Plagioclase-phyric basalt	BVL-0026A Plagioclase-phyric basalt	BVL-0026B Vesicular basalt	
Plagioclase	40	35	20	27	15	25	35	15	37	
Clinopyroxene	20		20	35	30		23		35	
Fe–Ti oxides	7	5	3	8	5	5	5	5	7	
Glass (devitrified)						40	15			
Sericite	3	10		10	25	17	7	40	5	
Amphibole	10	35								
Chlorite	20	15		15	25	3	5	25	10	
Biotite				5						
Calcite			3			10	10	5	4	
Epidote			54		tr			10		
Quartz					tr				2	
Sphene				tr						
Pyrite										
Hematite										
An content (mol%)										
Mean	56.71	57.46		4.60	11.17	1.78	2.11		21.69	
Range	42.23–67.55	51.25–65.06		2.94–7.88	4.16–21.99	0.40–5.83	1.24–3.34		14.02–51.93	
Cpx Mg# (range)	0.58–0.71			0.64–0.78	0.69–0.76				0.57	

Table 2

Major, trace and REE for the Punagarh and Sindreth rocks.

Location and sample	Delhi Supergroup									
	28 (quartz diorite/tonalite)	29 (diorite/tonalite)	30 (granite)	52 (dacite)	53 (agglomerate)	54 (basalt)	55 (dacite)	56 (dacite)		
SiO ₂	69.51	54.75	67.08	63.68	78.34	40.53	62.17	41.30		
TiO ₂	0.87	1.39	0.56	1.32	0.74	3.47	0.76	2.90		
Al ₂ O ₃	13.32	17.14	14.79	13.97	12.39	14.83	14.53	14.70		
Fe ₂ O ₃ ^a	4.94	9.14	4.46	8.21	1.74	11.95	8.14	14.49		
MnO	0.04	0.16	0.09	0.11	0.02	0.15	0.05	0.20		
MgO	1.30	3.22	1.33	1.39	0.73	2.63	1.52	7.08		
CaO	3.66	6.94	2.11	1.45	0.28	9.90	0.56	5.48		
Na ₂ O	5.63	3.82	3.97	2.97	0.05	2.96	4.80	3.02		
K ₂ O	0.08	1.76	3.78	4.35	4.02	2.23	2.91	0.81		
P ₂ O ₅	0.20	0.32	0.18	0.24	0.17	0.84	0.16	0.58		
SO ₃	0	0	0	0	0	0.05	0	0.17		
H ₂ O [−]	0.13	0.14	0.27	0.26	0.17	0.16	0.35	0.23		
LOI	1.30	2.07	1.99	1.95	2.31	9.81	2.40	8.51		
Total	100.98	100.84	100.62	99.90	100.95	99.51	98.35	99.46		
Sc	14.7	19.3	6.10	10.1	9.73	26.9	13.0	25.3		
V	38.9	202	51.4	88.1	73.9	238	1.02	198		
Cr	8.67	13.3	10.4	17.0	77.6	181	3.07	161		
Co	6.37	22.0	8.14	11.5	2.43	38.9	2.37	44.9		
Ni	8.67	9.97	6.37	7.23	14.0	58.2	2.87	72.5		
Cu	7.58	38.3	731	17.0	24.7	22.2	21.6	40.9		
As	0.88	0.80	1.70	8.44	7.42	13.7	3.66	14.2		
Rb	0.43	43.5	102	123	219	162	91.9	70.0		
Sr	126	423	239	111	18.5	154	87.0	118		
Y	129	25.4	18.4	80.6	33.6	35.5	101	36.2		
Zr	872	57.0	92.9	491	232	332	1914	279		
Nb	33.1	7.88	8.71	51.9	14.7	20.3	47.7	17.9		
Cs	0.08	2.44	1.68	3.59	13.1	19.8	2.35	7.22		
Ba	13.2	349	1004	339	476	275	513	112		
La	26.6	18.3	26.1	88.2	44.9	36.8	106	27.1		
Ce	72.2	47.0	55.9	214	85.1	75.9	209	61.9		
Pr	10.7	5.81	6.07	23.6	10.4	9.67	28.4	8.14		
Nd	52.6	24.9	22.3	91.7	38.0	40.9	116	34.7		
Sm	15.4	5.53	3.95	18.3	7.36	8.46	24.0	7.77		
Eu	3.96	1.56	1.04	2.17	1.31	3.06	4.80	2.46		
Gd	18.8	5.47	3.73	16.8	6.61	8.22	23.0	7.86		
Tb	3.37	0.85	0.56	2.67	1.01	1.19	3.44	1.20		
Dy	22.4	5.04	3.29	15.5	5.92	6.61	19.5	6.94		
Ho	4.82	1.00	0.68	3.10	1.14	1.28	3.92	1.39		
Er	15.0	2.82	2.02	9.02	3.31	3.49	11.2	3.78		
Tm	2.21	0.39	0.29	1.27	0.48	0.46	1.62	0.53		
Yb	14.8	2.50	1.98	8.23	3.21	2.94	11.0	3.32		
Lu	2.22	0.37	0.32	1.22	0.49	0.43	1.72	0.50		
Hf	22.3	2.03	3.09	13.6	6.66	6.55	37.8	6.25		
Ta	2.38	0.66	0.74	3.20	1.40	1.23	2.98	1.42		
Pb	2.50	10.4	12.1	12.1	7.77	7.77	170	5.59		
Th	8.02	5.23	9.52	21.6	20.2	2.25	17.73	3.23		
U	1.60	1.25	1.89	2.52	3.31	0.45	3.27	0.68		
K	648	14,569	31,380	36,136	33,405	18,504	24,116	6,708		
Ti	5192	8,357	3,369	7,919	4,412	20,791	4,538	17,356		
P	886	1,388	790	1,056	751	3,648	707	2,523		
[La/Yb] _N	1.79	7.34	13.2	10.7	14.0	12.5	9.60	8.15		
[La/Lu] _N	12.0	49.0	81.9	72.2	91.6	85.0	61.7	53.7		
Mg# ^b	21	26	23	14	30	18	16	33		
Location and sample	Punagarh Group									
	5A (basalt)	5B (dacite)	5C (basalt)	7 (volcanic breccia)	8A (basalt)	8B (basalt)	8C (basalt)	8D (pillow rim)	9A (dolerite)	9B (basalt)
SiO ₂	48.29	64.86	48.25	42.45	46.96	47.47	47.38	47.63	53.01	51.21
TiO ₂	1.99	1.07	2.15	2.22	2.15	2.20	2.08	2.16	1.23	1.15
Al ₂ O ₃	12.91	14.15	14.37	13.51	14.39	14.82	14.63	14.72	16.25	16.44
Fe ₂ O ₃ ^a	12.68	5.69	13.38	12.51	14.39	13.14	13.46	13.02	9.30	9.15
MnO	0.19	0.19	0.19	0.23	0.19	0.19	0.20	0.17	0.14	0.15
MgO	3.79	2.26	4.86	5.19	4.36	4.83	4.92	4.34	5.66	6.38
CaO	10.01	1.99	7.42	9.21	10.19	10.35	11.84	12.07	7.87	7.19
Na ₂ O	3.37	5.33	4.33	4.34	3.23	2.75	2.18	2.72	3.05	3.91
K ₂ O	2.20	2.01	0.46	0.56	1.11	1.74	0.45	0.32	1.23	1.03
P ₂ O ₅	0.24	0.35	0.23	0.31	0.23	0.24	0.23	0.24	0.19	0.18
SO ₃	0	0	0.08	0	0	0	0	0	0	0
H ₂ O [−]	0.29	0.37	0.34	0.72	0.31	0.21	0.25	0.32	0.19	0.19
LOI	3.92	2.40	3.99	8.71	2.54	2.13	2.24	1.74	2.34	2.95

Table 2 (Continued)

Location and sample	Punagarh Group										
	5A (basalt)	5B (dacite)	5C (basalt)	7 (volcanic breccia)	8A (basalt)	8B (basalt)	8C (basalt)	8D (pillow rim)	9A (dolerite)	9B (basalt)	
Total	99.87	100.66	100.05	99.97	100.05	100.06	99.86	99.45	100.46	99.93	
Sc	36.4	15.7	38.5	37.5	35.7	45.2	41.7	41.6	28.7	28.4	
V	313	57.5	331	309	336	346	321	336	222	205	
Cr	153	4.38	159	171	162	174	164	170	128	158	
Co	41.2	7.61	43.8	34.7	45.2	50.5	48.7	41.2	31.6	32.5	
Ni	36.6	2.50	44.0	27.5	35.4	45.7	47.9	39.3	25.1	30.1	
Cu	27.0	13.2	30.8	26.5	26.9	31.8	34.5	30.6	12.7	8.13	
As	1.14	1.83	1.60	2.11	1.10	1.67	1.30	1.50	1.16	1.01	
Rb	40.9	31.5	6.43	8.07	23.1	49.5	12.0	7.37	32.0	29.0	
Sr	253	139	269	81.6	168	181	144	171	276	308	
Y	38.3	31.5	40.0	40.3	39.5	43.8	42.1	42.7	25.3	20.6	
Zr	139	252	149	147	148	150	143	149	140	105	
Nb	6.94	8.87	7.42	7.27	7.48	7.31	7.26	7.56	9.95	7.82	
Cs	0.48	0.43	0.53	0.49	0.70	1.00	0.47	0.76	1.05	0.92	
Ba	440	877	145	201	196	308	181	319	328	214	
La	8.17	23.9	8.55	8.92	8.54	10.8	10.5	10.2	18.2	13.9	
Ce	21.8	63.4	23.8	23.9	23.8	26.4	25.3	25.7	37.7	30.8	
Pr	3.05	7.48	3.22	3.10	3.23	3.69	3.59	3.65	4.35	3.55	
Nd	15.2	31.0	15.7	15.2	16.0	17.9	17.2	17.8	17.5	14.7	
Sm	4.58	6.40	4.71	4.38	4.77	5.24	5.03	5.15	3.76	3.26	
Eu	1.51	1.57	1.51	1.55	1.62	1.91	1.70	1.77	1.25	1.13	
Gd	5.79	6.33	5.99	6.02	5.96	7.04	6.27	6.55	4.27	3.69	
Tb	1.01	0.98	1.04	1.06	1.03	1.20	1.07	1.11	0.71	0.60	
Dy	6.56	5.88	6.89	6.91	6.69	7.74	7.00	7.15	4.40	3.73	
Ho	1.37	1.19	1.45	1.49	1.42	1.61	1.47	1.52	0.92	0.80	
Er	4.03	3.46	4.24	4.45	4.14	4.71	4.22	4.34	2.72	2.31	
Tm	0.57	0.48	0.61	0.64	0.59	0.66	0.60	0.62	0.39	0.33	
Yb	3.68	3.11	3.91	4.07	3.87	4.30	3.95	4.01	2.56	2.23	
Lu	0.56	0.47	0.60	0.62	0.58	0.65	0.60	0.61	0.39	0.33	
Hf	3.50	6.82	3.79	3.83	3.71	3.81	3.58	3.74	3.31	2.66	
Ta	0.46	0.71	0.49	0.59	0.48	0.57	0.47	0.48	0.73	0.64	
Pb	1.92	18.9	2.93	1.57	1.34	1.99	1.57	2.19	3.49	1.72	
Th	1.39	6.75	1.46	1.53	1.48	1.64	1.58	1.64	4.50	3.11	
U	0.22	1.37	0.28	0.31	0.26	0.29	0.28	0.27	1.01	0.58	
K	18,230	16,686	3,835	4,682	9,173	14,445	3,769	2,648	10,244	8534	
Ti	11,924	6,415	12,913	13,291	12,913	13,195	12,452	12,973	7,398	6894	
P	1,034	1,527	1,021	1,340	1,012	1,065	1,004	1,056	820	781	
[La/Yb] _N	2.22	7.68	2.18	2.19	2.21	2.50	2.66	2.55	7.10	6.23	
[La/Lu] _N	14.7	10.5	14.2	14.4	14.7	16.6	17.4	16.9	46.2	41.7	
Mg# ^b	23	48.1	27	29	23	27	27	25	38	41	
Location and sample	Punagarh Group										
	14B (dolerite)	15 (dolerite)	16 (dolerite)	18 (diorite)	19 (basalt)	20 (dolerite/gabbro)	22A (f.g. volcanic rock)	24A (basalt)	24B (basalt)	26A (basalt)	26B (basalt)
SiO ₂	47.45	48.43	48.31	48.03	48.24	49.03	79.12	47.29	45.90	38.64	52.93
TiO ₂	1.50	2.17	1.71	1.34	2.39	2.11	0.17	2.01	1.82	1.06	1.22
Al ₂ O ₃	14.52	14.81	15.63	15.03	13.68	14.08	11.66	12.88	11.72	12.35	14.95
Fe ₂ O ₃ ^a	8.73	13.69	12.88	10.08	12.29	11.92	1.91	12.52	10.91	9.64	10.10
MnO	0.20	0.25	0.21	0.18	0.33	0.21	0.07	0.17	0.16	0.14	0.15
MgO	6.22	6.91	7.92	4.95	6.34	6.17	0.45	3.33	3.42	4.05	3.95
CaO	7.21	9.54	9.92	15.92	8.40	9.53	0.26	7.99	13.24	21.15	8.91
Na ₂ O	3.18	2.32	2.27	1.70	3.86	3.29	5.52	5.48	4.86	1.40	2.22
K ₂ O	1.60	0.61	0.32	0.07	0.59	0.97	1.00	0.49	0.81	0.08	1.67
P ₂ O ₅	0.28	0.22	0.18	0.15	0.30	0.27	0.02	0.22	0.24	0.16	0.12
SO ₃	0	0	0	0	0	0	0	0	0	0	0
H ₂ O ⁻	0.27	0.10	0.06	0.24	0.53	0.32	0.12	0.21	0.18	0.28	0.26
LOI	8.60	1.08	0.74	2.06	2.80	1.94	0.65	7.14	6.52	10.33	3.45
Total	99.76	100.12	100.15	99.75	99.74	99.85	100.94	99.73	99.78	99.27	99.93
Sc	26.4	40.0	35.2	38.2	46.2	46.5	4.14	35.6	36.5	31.6	33.2
V	255	318	271	260	355	345	15.9	306	269	225	239
Cr	192	173	124	256	223	200	17.4	154	144	220	231
Co	32.1	47.2	50.2	29.0	37.8	39.3	1.58	36.0	35.3	39.1	37.5
Ni	88.6	52.3	73.6	50.1	32.6	34.1	7.79	38.1	34.7	44.3	52.7
Cu	50.9	17.5	34.9	32.4	52.7	62.7	16.4	24.5	33.0	12.4	17.9
As	4.45	2.83	1.06	0.69	1.22	1.21	1.46	1.79	1.22	1.31	0.94
Rb	57.6	17.3	7.20	1.06	12.2	24.3	19.8	9.01	18.6	1.20	78.8
Sr	484	214	181	406	222	274	93.8	255	110	96.9	182
Y	23.9	32.9	27.9	26.3	36.3	34.4	31.8	34.9	36.1	22.3	28.0
Zr	192	121	91.8	78.2	149	144	128	142	127	66.6	114
Nb	7.55	9.19	7.81	6.05	11.7	10.7	10.7	6.93	6.37	3.44	7.41

Table 2 (Continued)

Location and sample	Punagarh Group										
	14B (dolerite)	15 (dolerite)	16 (dolerite)	18 (diorite)	19 (basalt)	20 (dolerite/gabbro)	22A (f.g. volcanic rock)	24A (basalt)	24B (basalt)	26A (basalt)	26B (basalt)
Cs	5.04	1.58	1.56	0.10	0.80	1.41	0.51	1.45	0.19	0.10	3.32
Ba	1508	123	70.8	19.0	1109	223	565	326	115	21.1	210
La	19.2	9.00	7.01	10.3	9.89	8.93	26.4	7.27	8.84	6.89	17.6
Ce	47.3	21.7	17.7	23.1	25.1	23.6	52.9	21.4	21.9	15.4	37.3
Pr	6.19	3.06	2.51	3.03	3.62	3.38	6.00	2.85	3.10	2.07	4.45
Nd	26.8	14.7	12.4	13.7	17.6	16.4	22.3	14.1	15.3	9.47	18.0
Sm	5.44	4.14	3.51	3.66	5.11	4.71	5.02	4.20	4.42	2.62	4.05
Eu	1.79	1.62	1.46	1.31	2.01	1.82	0.66	1.37	1.41	1.04	1.21
Gd	5.30	5.47	4.62	4.44	6.31	6.01	5.05	5.34	5.49	3.29	4.29
Tb	0.79	0.92	0.78	0.75	1.06	1.01	0.87	0.93	0.94	0.58	0.73
Dy	4.42	5.80	4.95	4.73	6.67	6.40	5.62	6.11	6.06	3.66	4.61
Ho	0.86	1.21	1.03	0.99	1.36	1.30	1.20	1.29	1.26	0.77	0.98
Er	2.37	3.53	2.97	2.84	3.93	3.77	3.70	3.77	3.63	2.23	2.89
Tm	0.32	0.49	0.42	0.40	0.54	0.52	0.56	0.53	0.51	0.32	0.42
Yb	2.06	3.21	2.68	2.56	3.49	3.36	3.84	3.46	3.37	2.10	2.75
Lu	0.31	0.48	0.41	0.39	0.52	0.50	0.59	0.53	0.51	0.32	0.42
Hf	5.09	3.04	2.29	2.21	3.55	3.43	4.33	3.54	3.21	1.66	2.97
Ta	0.57	0.67	0.59	0.49	0.87	0.77	1.01	0.44	0.41	0.30	0.59
Pb	28.7	2.85	2.27	9.17	2.69	2.21	15.2	5.38	1.96	3.78	15.3
Th	3.48	1.23	0.91	2.37	1.11	1.08	17.2	1.27	1.36	0.92	6.44
U	0.75	0.30	0.23	0.59	0.28	0.28	3.78	0.22	0.20	0.13	1.10
K	13,249	5,097	2,623	606	4865	8061	8268	4,059	6,691	656	13,855
Ti	8,993	12,997	10,263	8021	14,322	12,673	1025	12,032	10,905	6367	7,284
P	1,235	938	781	668	1,296	1,196	105	978	1,030	716	537
[La/Yb] _N	9.34	2.81	2.62	4.01	2.83	2.65	6.86	2.10	2.62	3.28	6.41
[La/Lu] _N	62.9	18.6	17.3	26.6	19.1	18.0	45.0	13.8	17.3	21.8	42.3
Mg# ^b	42	34	38	33	34	34	19	21	24	30	28
Location and sample	Sindreh Group										
	37A (basalt)	37B (dacite)	38 (basalt)	43 (silicic tuff)	46A (basalt)	46B (basalt)	46C (basalt)	46D (basalt)	46E (basalt)	46F (basalt)	
SiO ₂	43.91	64.50	51.66	74.85	45.36	44.96	49.41	45.33	44.35	50.67	
TiO ₂	2.64	0.88	1.96	0.40	2.60	2.89	2.88	2.72	3.03	2.93	
Al ₂ O ₃	12.25	13.18	16.82	13.04	13.68	14.31	14.21	15.69	14.93	13.00	
Fe ₂ O ₃ ^a	17.48	7.13	13.21	2.71	12.00	12.97	11.04	13.25	13.69	10.11	
MnO	0.22	0.09	0.11	0.07	0.19	0.17	0.16	0.20	0.24	0.14	
MgO	1.93	0.61	1.16	0.58	4.20	4.38	3.70	4.64	5.77	3.08	
CaO	8.27	2.95	5.89	0.76	8.61	8.19	6.05	8.86	6.99	8.04	
Na ₂ O	0.11	2.77	6.71	6.69	2.64	3.13	4.64	2.53	3.35	4.25	
K ₂ O	1.86	4.99	0.03	0.20	1.02	0.49	0.11	0.23	0.17	0.07	
P ₂ O ₅	1.96	0.33	0.20	0.15	0.68	0.72	0.74	0.44	0.52	0.76	
SO ₃	0	0	0	0	0	0	0	0	0	0	
H ₂ O ⁻	0.82	0.24	0.42	0.19	0.07	0.15	0.12	0.10	0.22	0.36	
LOI	8.37	3.23	1.51	1.33	8.83	7.37	6.60	5.01	6.69	6.70	
Total	99.82	100.89	99.67	100.96	99.87	99.72	99.66	98.99	99.94	100.10	
Sc	29.8	10.4	26.5	7.38	22.4	23.5	19.7	27.0	25.8	18.1	
V	55.5	21.0	188	16.9	182	199	166	249	246	148	
Cr	3.66	6.27	99.4	11.7	127	159	162	56.0	57.6	80.6	
Co	23.8	6.86	20.5	1.92	40.6	41.4	39.4	47.9	50.2	31.8	
Ni	3.45	3.97	22.7	7.14	55.1	62.8	69.4	38.3	48.8	36.7	
Cu	17.0	12.6	11.3	7.49	28.3	16.0	31.3	21.8	16.8	20.1	
As	6.66	1.92	3.59	4.08	2.84	2.04	1.59	7.77	2.47	6.38	
Rb	46.1	170	0.30	6.79	48.7	22.5	2.75	6.71	4.22	1.60	
Sr	61.1	60.8	909	82.4	256	360	344	771	306	295	
Y	96.2	59.5	22.8	28.5	38.1	38.6	32.3	30.6	33.4	37.2	
Zr	762	575	183	192	303	344	335	220	265	350	
Nb	33.1	33.8	15.5	5.07	20.7	23.9	23.4	19.1	19.4	22.4	
Cs	4.18	1.56	0.02	0.39	1.07	0.72	0.75	0.30	0.23	0.57	
Ba	248	659	34.7	155	138	144	78.5	77.5	63.4	66.1	
La	70.3	71.4	15.3	40.3	30.9	30.6	20.8	20.4	20.5	31.7	
Ce	169	161	36.0	83.5	69.8	71.0	55.4	47.1	49.3	77.1	
Pr	22.8	18.5	4.72	9.90	8.96	9.14	6.62	6.21	6.56	9.44	
Nd	101	71.4	20.6	41.3	38.0	38.8	29.5	26.9	28.9	40.1	
Sm	22.3	14.5	4.68	8.11	8.23	8.45	6.94	6.08	6.55	8.80	
Eu	5.65	2.31	1.74	1.80	2.46	2.23	2.24	2.23	2.27	2.59	
Gd	22.0	13.2	4.76	6.95	8.07	8.18	6.94	6.30	6.84	8.28	
Tb	3.27	2.03	0.74	0.97	1.20	1.23	1.06	0.95	1.04	1.25	
Dy	18.8	11.9	4.28	5.42	6.84	7.07	6.17	5.50	5.98	7.08	
Ho	3.71	2.34	0.83	1.05	1.32	1.37	1.20	1.08	1.18	1.36	
Er	10.3	6.73	2.26	3.06	3.59	3.72	3.29	2.94	3.22	3.69	
Tm	1.39	0.93	0.31	0.45	0.48	0.51	0.45	0.40	0.43	0.49	

Table 2 (Continued)

Location and sample	Sindreh Group									
	37A (basalt)	37B (dacite)	38 (basalt)	43 (silicic tuff)	46A (basalt)	46B (basalt)	46C (basalt)	46D (basalt)	46E (basalt)	46F (basalt)
Yb	8.58	5.98	1.96	2.92	3.07	3.22	2.85	2.56	2.77	3.15
Lu	1.29	0.87	0.29	0.45	0.45	0.48	0.42	0.38	0.40	0.46
Hf	16.5	13.8	3.98	5.16	6.31	7.06	6.91	4.84	5.59	7.36
Ta	2.22	1.90	0.96	0.48	1.39	1.48	1.47	1.18	1.20	1.37
Pb	17.5	6.82	8.61	12.3	8.18	8.89	4.53	4.86	5.62	4.08
Th	8.92	24.1	1.83	4.71	4.55	3.65	3.07	1.80	2.07	4.37
U	2.13	3.43	0.69	1.37	1.38	1.01	0.63	0.57	0.39	1.12
K	15,466	41,424	224	1660	8,426	4,076	938	1,868	1,386	589
Ti	15,815	5,276	11,726	2398	15,605	17,296	17,278	16,318	18,183	17,553
P	8,549	1,440	886	655	2,959	3,138	3,238	1,898	2,261	3,321
[La/Yb] _N	8.20	11.9	7.83	13.8	10.1	9.52	7.30	7.99	7.42	10.1
[La/Lu] _N	54.3	9.8	52.6	20.5	68.6	64.4	49.3	54.4	51.0	69.0
Mg# ^b	10	16.6	8	33.3	26	25	25	26	30	23
Location and sample	Sindreh Group									
	47A (dolerite)		47B (rhyolite)		48 (basalt)		49 (basalt)		57 (rhyolite)	
SiO ₂	43.42		69.37		46.65		44.12		79.27	
TiO ₂	2.94		0.42		3.05		3.18		0.07	
Al ₂ O ₃	15.22		13.99		15.46		15.31		12.13	
Fe ₂ O ₃ ^a	13.75		4.54		14.90		14.57		0.58	
MnO	0.20		0.04		0.21		0.20		0	
MgO	3.93		1.02		4.38		4.08		0	
CaO	9.07		0.51		5.15		5.67		0.09	
Na ₂ O	2.71		2.21		3.28		4.65		4.32	
K ₂ O	0.50		6.65		2.16		0.74		3.92	
P ₂ O ₅	0.52		0.11		0.62		0.80		0.01	
SO ₃	0		0		0		0		0	
H ₂ O ⁻	0.12		0.17		0.17		0.24		0.15	
LOI	7.14		1.70		4.01		6.43		0.32	
Total	99.53		100.72		100.03		100.00		100.87	
Sc	24.5		2.56		23.0		24.9		0.26	
V	241		10.9		233		216		4.74	
Cr	53.5		7.42		57.7		140		9.83	
Co	47.6		2.46		38.8		41.6		0.77	
Ni	49.4		4.24		44.2		57.7		5.06	
Cu	22.0		5.65		19.1		15.1		8.64	
As	3.69		1.26		3.73		2.37		0.99	
Rb	12.5		281		32.7		26.3		197	
Sr	752		33.0		421		212		29.7	
Y	33.2		68.7		39.5		38.7		66.3	
Zr	254		237		385		362		144	
Nb	20.6		27.1		26.0		25.0		26.2	
Cs	0.56		2.54		0.76		0.57		0.79	
Ba	123		315		1265		125		71.9	
La	25.0		93.4		25.3		28.8		24.9	
Ce	58.2		187		65.8		74.4		60.2	
Pr	7.44		22.5		8.13		9.14		7.66	
Nd	32.1		80.4		35.5		40.5		34.0	
Sm	7.03		15.2		8.01		8.86		11.1	
Eu	2.59		1.43		2.44		2.90		0.75	
Gd	7.10		14.0		8.19		8.68		12.4	
Tb	1.07		2.23		1.27		1.29		2.23	
Dy	6.11		13.0		7.39		7.32		14.1	
Ho	1.17		2.61		1.45		1.43		2.87	
Er	3.27		7.35		4.06		3.91		9.04	
Tm	0.44		1.06		0.55		0.52		1.50	
Yb	2.75		6.55		3.46		3.34		10.2	
Lu	0.40		0.96		0.51		0.49		1.50	
Hf	5.41		7.40		8.06		7.51		7.23	
Ta	1.33		2.22		1.59		1.55		2.74	
Pb	4.79		3.95		8.24		5.63		4.33	
Th	2.08		45.3		3.10		3.69		53.7	
U	0.45		4.05		0.79		1.01		7.21	
K	4,167		55,205		17,923		6,168		32,542	
Ti	17,625		2,518		18,285		19,058		420	
P	2,274		480		2,697		3,496		44	
[La/Yb] _N	9.08		14.3		7.32		8.61		2.43	
[La/Lu] _N	62.5		10.2		49.5		58.6		16.6	
Mg# ^b	22		34.4		23		22		0.0	

^a Total Fe as Fe₂O₃.^b Mg# = 100[Fe/(Fe + Mg)].

(3.00–10.00 wt.%), with the rest of the oxides showing values similar to alkali basalt whole-rock analyses. In greenschist-facies rocks, epidote is characteristically associated with chlorite, actinolite, albite and quartz, as can be seen in some of the studied samples (BVL-005, 0020, 0024 and 0046). The actinolite associated with the chlorite and epidote is mainly Mg-rich (avg. $\text{Mg}/\text{Mg} + \text{Fe} = 0.453 \pm 0.24$, $n = 16$). Other secondary effects include the oxidation of ilmenite and magnetite to hematite, the growth of secondary quartz and the surrounding of plagioclase laths with

actinolite (alteration of clinopyroxene). Calcite, as a secondary Ca-bearing phase, is generally rare in these specimens.

The felsic volcanic rocks from the Sindreth Group include dacite and rhyolite (BVL-0037A, 0044, 0047B and 0057). The dacite consists of altered K-feldspar and plagioclase phenocrysts (altered to sericite), quartz, opaques and chlorite, in a fine-grained matrix. The rhyolites consist of phenocrysts of quartz and plagioclase, K-feldspar, opaques and secondary chlorite. The quartz phenocrysts of one of the rhyolites (BVL-0057) are commonly embayed.

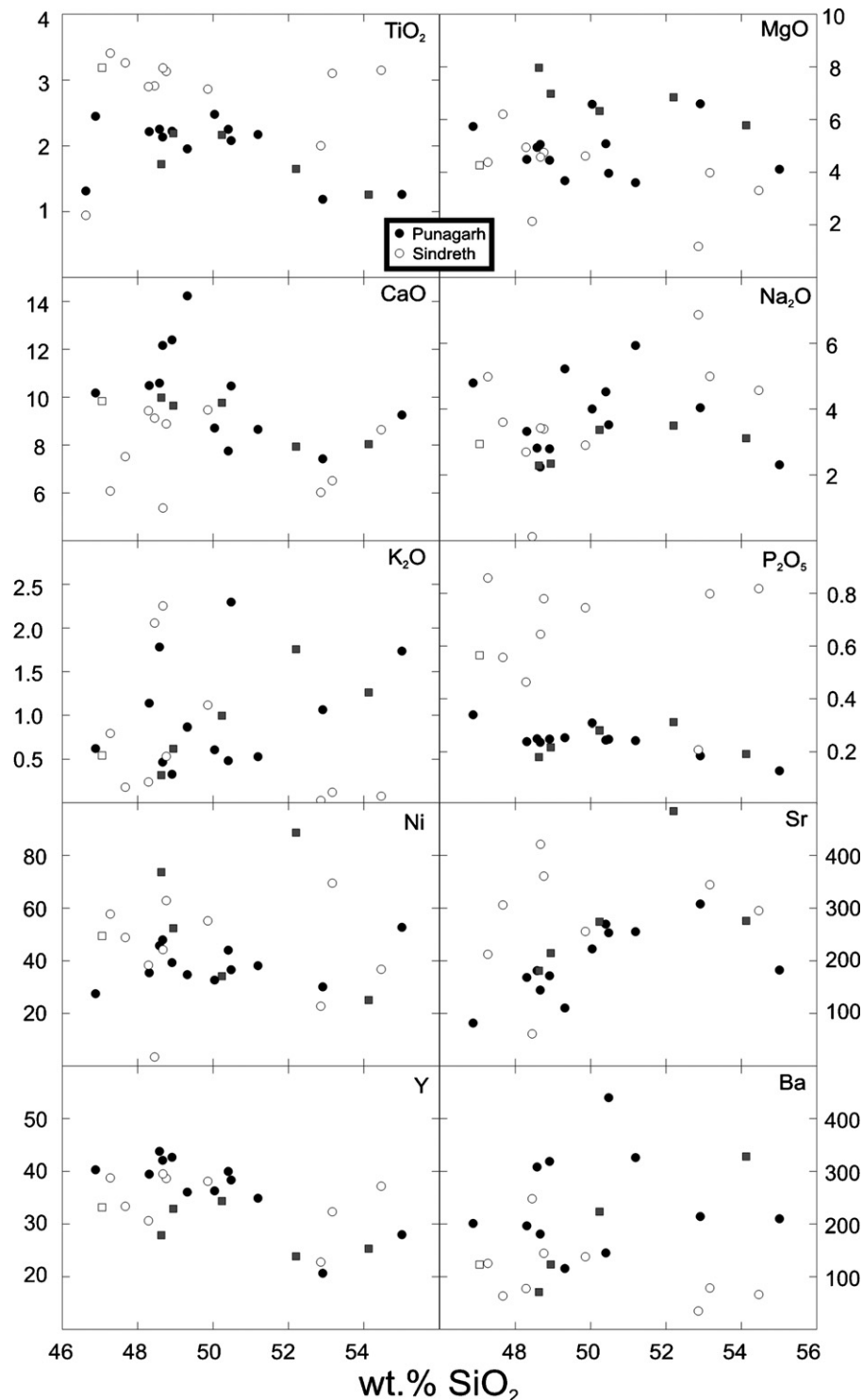


Fig. 6. Whole-rock compositions (recalculated to 100% volatile-free) of Punagarh and Sindreth mafic rocks (basalts and dolerites) plotted on a series of Harker diagrams. Major element oxide abundances are plotted in wt.%, and trace element concentrations are shown as ppm.

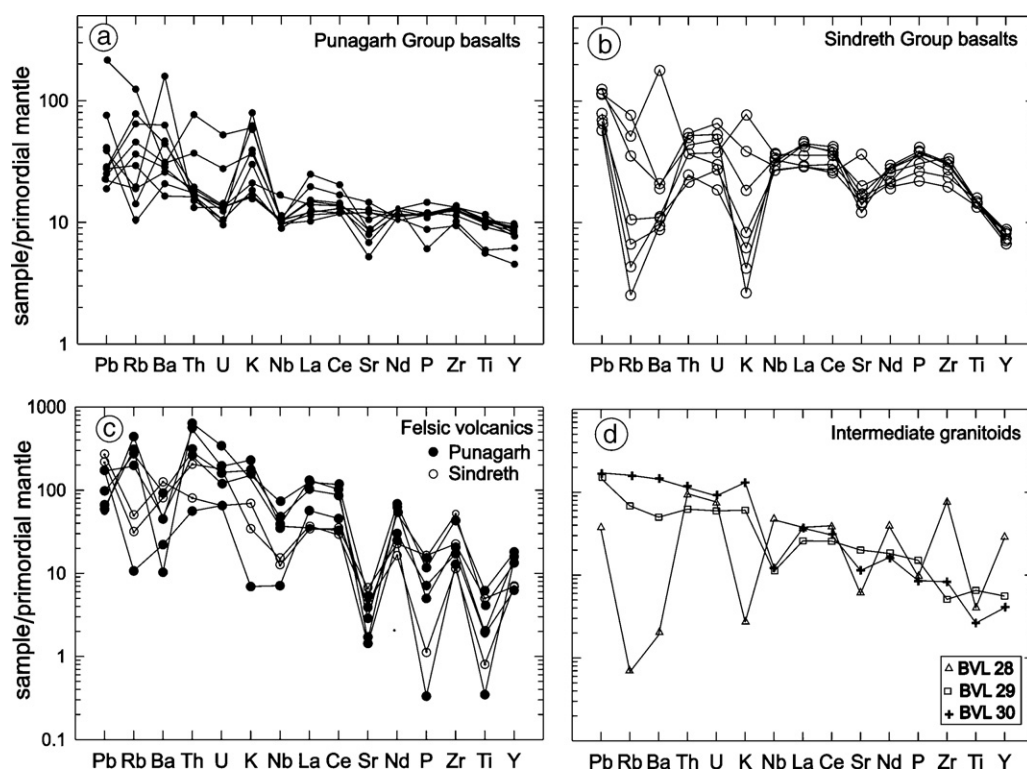


Fig. 7. Normalized multi-element (spider) diagrams comparing trace element concentrations of (a) Punagarh Group basalts, (b) Sindreth Group basalts, (c) Punagarh and Sindreth felsic volcanics and (d) intermediate granitoids. Data are normalized to primordial mantle values of Sun (1982).

Tonalite, along with pink granite and granitic gneiss forms the basement for the Punagarh rocks. Our sample of tonalite (BVL-0028) from the Punagarh area consists of 2–3 mm plagioclase laths surrounded by quartz and myrmekite/granophyre. Magmatic texture is well preserved, with large, primary epidote crystals (either euhedral, with square cross-sections, or filling interstitial patches, with euhedral inclusions of plagioclase), and very minor Fe–Ti oxides, zircon, apatite and biotite. The other plutonic rocks studied also have well preserved magmatic texture despite variable hydrothermal alteration, mainly represented by sericitization of feldspars. These include mafic tonalite BVL-0029 (but normatively a quartz monzodiorite), which contains about 17% hornblende and chloritized biotite, and muscovite-bearing granodiorite BVL-0030.

5.2. Whole-rock major and trace element geochemistry

Whole rock chemical analyses, including major, minor and trace element compositions, of the Punagarh and Sindreth Group rocks are given in Table 2.

Punagarh and Sindreth basalts and dolerites show a very large range in volatile content, expressed as loss on ignition (LOI). Punagarh samples vary from 0.74 to 10.33 wt.% LOI (avg. = 3.96; $n = 19$), whereas Sindreth samples contain overall higher LOI values 1.51–8.83 wt.% (avg. = 6.24 wt.%, $n = 11$). In order to approximate the primary compositions of these rocks, we recalculated their major element analyses on a 100% volatile-free basis (Fig. 6). On this basis, the average SiO_2 content, and range of values, of mafic rocks from the Punagarh ($\text{SiO}_2 = 49.88 \pm 2.58$ wt.%, $n = 19$) and Sindreth ($\text{SiO}_2 = 49.68 \pm 2.59$ wt.%, $n = 11$) Groups, are virtually identical. Doleritic rocks from the Punagarh Group show very similar major and trace element concentrations to the basalts; likewise a single dolerite from the Sindreth Group is compositionally similar to basaltic rocks from that area (Fig. 6).

Normative compositions (calculated on an anhydrous basis) indicate that the basalts from both the Punagarh and Sindreth

Groups are dominantly olivine tholeiites, although a few samples are quartz-normative and even fewer are nepheline-normative alkali basalts. In detail, there are some apparent differences between the two groups, with the Sindreth samples showing, for example, higher TiO_2 and P_2O_5 than those from Punagarh (Fig. 6). Such differences may be primary, although this is difficult to evaluate given the variable geochemical effects of hydrothermal alteration. Trace element differences between the two groups are apparent on normalized multi-element (spider) diagrams (Fig. 7a and b), which show that Sindreth basalts have overall higher concentrations of incompatible elements such as Pb, U and Th. In general, the patterns for Sindreth basalts are more variable than those of the Punagarh Group, although there is considerable overlap.

Despite these possible primary compositional features, it is important to keep in mind the profound, but variable secondary volatile enrichment of these rocks. There are correlations between LOI and some major element ratios (e.g. $\text{CaO}/\text{Na}_2\text{O}$, Fig. 8a) and trace element ratios (e.g. Nb/U , Nb/Th , Fig. 8b). We interpret this in terms of hydrothermal alteration processes, as discussed below.

The Punagarh basalts generally present flat REE slopes with small to insignificant negative Eu anomalies, whereas Sindreth basalts exhibit slight LREE enrichment, as illustrated in chondrite-normalized REE plots (Fig. 9a and b). The REE abundance levels of the Punagarh basalts decrease from La = 15–30 \times chondrites to Lu = 9–20 \times chondrites ($[\text{La}/\text{Lu}]_N = 1.5\text{--}1.7$). In contrast, the Sindreth basalts are defined by La = 45–80 \times chondrites to Lu = 10–15 \times chondrites ($[\text{La}/\text{Lu}]_N = 4.5\text{--}5.3$), also with negligible Eu anomalies.

Felsic volcanic rocks from the Punagarh and Sindreth areas are normatively dacites and rhyolites, with SiO_2 (recalculated anhydrous) varying between 65.03 and 79.55 wt.% (avg. = 71.82 ± 6.32 wt.%, $n = 9$). In general, these felsic rocks are less altered than the mafic volcanics, having LOI values between 0.47 and 3.47 wt.% (avg. = 2.03 ± 0.98 wt.%). Normalized trace element concentrations for the felsic volcanics show high variability (Fig. 7c),

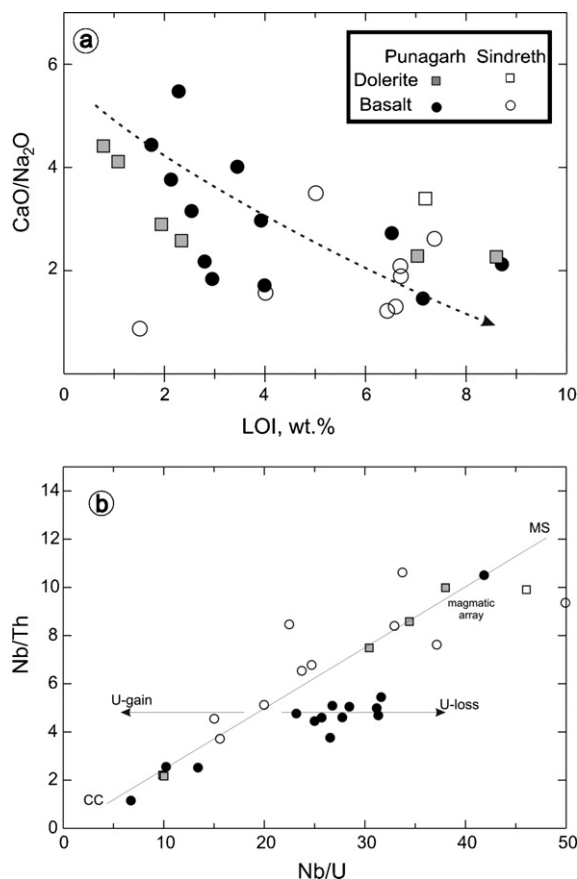


Fig. 8. (a) Plot of wt.% loss on ignition (LOI) vs. CaO/Na₂O, for mafic rocks (basalts and dolerites) from the Punagarh and Sindreth Groups. Dashed line with arrows illustrates our proposed trends of hydrothermal alteration involving progressive increases in volatile constituents. (b) Plot of Nb/Th vs. Nb/U showing magmatic array representing mixing between a putative mantle source (MS) and continental crust (CC). Effects of U-mobility shift points horizontally on this diagram, and are especially important for Punagarh basalts.

and cannot be clearly correlated with any of the major types of granitoids (A-, I- or S-types). For this and other reasons we choose not to attempt tectonic discrimination based on geochemistry. For the most part, the REE show uniform pattern shapes, with variable negative Eu anomalies (Fig. 9c); the rhyolitic rocks have more prominent Eu anomalies than the dacites.

The plutonic rocks that we studied are granitoids of intermediate composition, both modally and normatively, with anhydrous SiO₂ values between 54.75 and 69.57 wt.%. In terms of trace elements, samples BVL-0029 and -30 are geochemically similar, despite large differences in modal and normative % mafic minerals. These rocks show relatively smooth normalized LILE abundances (Fig. 7d) that lack the prominent negative anomalies, for example in Ba, as for the felsic volcanics discussed above. The REE patterns are also similar, with small negative Eu anomalies. Tonalite sample BVL-0028, collected from about 9 km NE of BVL-0020 and -30 (Fig. 2), is chemically distinct, with prominent depletions in Pb, Rb, Ba and K (Fig. 7d), and exhibits a flat REE pattern at about 60x chondrites, with a distinct negative Eu anomaly (Fig. 9d).

5.3. Geochronology and isotopic geochemistry

Analyses were carried out on air-abraded zircons from rhyolites and dacites from the Sindreth Group and granitoids pre-dating the Punagarh Group. The results are presented in Table 3 and are plotted on a series of concordia diagrams in Fig. 10. The ages discussed below are weighted mean ²⁰⁷Pb/²⁰⁶Pb ages.

The pre-Punagarh Group tonalite sample BVL-0028 contains prismatic and rounded (some broken) light yellow-brown zircons. BVL-0029, the mafic tonalite, contains clear euhedral or prismatic zircons. Sindreth rhyolite (BVL-0037B) yielded prismatic clear to light yellow coloured zircons, whereas rhyolite sample BVL-0047B contains euhedral and prismatic, clear to slightly discoloured, zircons. The rhyolitic dyke intrusive into the Sirohi Group phyllites (BVL-0052) yielded rounded to prismatic zircons that are clear to light yellow in colour. The Sindreth Group rhyolite (BVL-0057), contains rounded, euhedral and prismatic, light zircons, yellow-brown to darker grey-brown in colour.

The mafic tonalite (BVL-0029) collected from the post-Delhi granites type area (Fig. 1) yielded an age of 800 ± 2.4 Ma (2σ , 3 data points, MSWD = 0.07; Fig. 10a). The rhyolitic dyke cutting the Sirohi Group (BVL-0052, Fig. 1) is statistically concordant, yielding an age of 765.3 ± 7.8 Ma (2σ , 3 data points, MSWD = 0.27; Fig. 10b). Tonalite BVL-0028, collected from the Punagarh Group type area, produced variably discordant data points and a concordia upper intercept age of 873.1 ± 2.6 Ma (2σ , 3 data points, MSWD = 0.19; Fig. 10c).

The first precise U–Pb zircon ages (this study) for the Sindreth Group felsic volcanics include an age of 767 ± 2.9 Ma for rhyolite sample BVL-0037B (2σ , 2 data points, MSWD = 0), and two ages for rhyolites from the overlying Angor Formation, yielding 765.9 ± 1.6 Ma for BVL-0047B (2σ , 3 data points, MSWD = 0.27; Fig. 10e) and 761 ± 16 Ma for BVL-0057 (2σ , 2 data points, MSWD = 0; Fig. 10e).

Sm–Nd isotopic data for selected Punagarh and Sindreth Group mafic and felsic rocks (Table 4) were obtained to constrain their isotopic signatures and evolution. Due to limited spread in ¹⁴⁷Sm/¹⁴⁴Nd and variable initial Nd ratios, no isochron relationships are apparent from these data, and we rely upon the U–Pb zircon results for age information.

Initial Nd ratios (expressed as ϵ_{Nd} values) were calculated at 765 Ma, representing our best estimate of the time of eruption of both the Punagarh and Sindreth volcanic rocks (Table 4). Punagarh mafic metavolcanic rocks vary in $\epsilon_{Nd,765}$ from +1.64 to +2.76. The dolerites extend this range to higher values, up to $\epsilon_{Nd,765} = +5.18$; the lowest $\epsilon_{Nd,765}$ of 0.94 is from a dacitic volcanic rock. Depleted mantle model ages range from 967 to 1906 Ma, with the dolerite giving the youngest model age. Sindreth metabasalts show a much wider range initial Nd ratios that extends to lower values ($\epsilon_{Nd,765} = -2.11$ to +3.56); values for a dolerite (+2.56) and a rhyolite (–1.89) are within this range. Depleted mantle model ages for Sindreth rocks vary from 1047 to 1851 Ma (Table 4).

6. Discussion and implications

6.1. Evidence for ocean-floor hydrothermal alteration effects

The mafic volcanic rocks of the Punagarh and Sindreth Groups share many, if not all of the features of hydrothermally altered basalts. Specifically these include the generally high degree of low-grade alteration in rocks showing the presence of identifiable pillow structures, well-preserved igneous textures including amygdalae, vesicles and elongate, randomly distributed microphe-nocrysts of plagioclase. The presence of albitic compositions in many microphe-nocrysts is characteristic of hydrothermally altered basaltic rocks, but in some of our samples apparently primary intermediate to calcic plagioclase is still partly preserved, suggesting that hydrothermal alteration has affected these rocks to a variable degree. These rocks also contain abundant chlorite, calcite and epidote, which is typical of hydrothermally altered basalts.

The variable (in some cases total) replacement of primary intermediate to calcic plagioclase (An_{44–67}) by secondary albite (An_{0.4–10.0}), and much of the original clinopyroxene and glass by

Table 3

U–Pb data for felsic rocks in the Punagarh and Sindreth Groups and the underlying Delhi Supergroup.

Sample fractions	Weight (μg)	Concentrations		²⁰⁶ Pb/ ²⁰⁴ Pb	²⁰⁸ Pb/ ²⁰⁶ Pb	²⁰⁶ Pb/ ²³⁸ U	% err	²⁰⁷ Pb/ ²³⁵ U	% err	²⁰⁷ Pb/ ²⁰⁶ Pb	% err	Age (Ma)			Corr. coef.
		U (ppm)	Pb (ppm)	(a)	(b)	(c)	(d)	(c)	(d)	(c)	(d)	²⁰⁶ Pb/ ²³⁸ U	²⁰⁷ Pb/ ²³⁵ U	²⁰⁷ Pb/ ²⁰⁶ Pb	
BVL-0028															
z1	0.8	283	68.6	1408.0	0.900	0.142583	(.16)	1.3369	(.30)	0.06800	(.24)	859.3	861.9	868.6	0.594
z2	0.7	440	111.7	1892.5	0.948	0.146092	(.14)	1.3744	(.20)	0.06823	(.14)	879.0	878.0	875.6	0.735
z3	1.1	345	77.9	1554.0	0.741	0.144724	(.16)	1.3593	(.20)	0.06812	(.11)	871.3	871.5	872.2	0.834
BVL-0029															
z1	2.7	146	23.7	1462.6	0.357	0.132732	(.16)	1.2044	(.29)	0.06581	(.23)	803.4	802.6	800.3	0.596
z2	2.0	210	36.6	478.7	0.372	0.132369	(.47)	1.2012	(.51)	0.06582	(.20)	801.4	801.2	800.6	0.923
z3	1.5	171	27.8	708.1	0.369	0.132007	(.30)	1.1973	(.35)	0.06578	(.18)	799.3	799.3	799.5	0.861
BVL-0037B															
z1	3.0	52	9.2	1288.5	0.571	0.126326	(.18)	1.1288	(.25)	0.06481	(.16)	766.9	767.2	768.0	0.770
z2	3.3	47	8.2	266.3	0.464	0.126107	(1.32)	1.1267	(1.47)	0.06480	(.59)	765.6	766.2	767.8	0.916
BVL-0047B															
z1	3.0	128	19.9	5847.1	0.373	0.125451	(.10)	1.1197	(.14)	0.06474	(.09)	761.9	762.9	765.7	0.755
z2	3.8	33	5.1	1108.3	0.388	0.125808	(.21)	1.1227	(.29)	0.06472	(.19)	763.9	764.3	765.3	0.756
z3	1.6	108	17.2	2569.0	0.396	0.126258	(.12)	1.1278	(.26)	0.06479	(.22)	766.5	766.7	767.4	0.545
BVL-0052															
z1	2.7	55	8.5	343.0	0.354	0.126232	(1.41)	1.1251	(1.53)	0.06464	(.56)	766.3	765.4	762.7	0.931
z2	3.3	42	6.5	321.4	0.337	0.125639	(1.48)	1.1210	(1.59)	0.06471	(.50)	762.9	763.4	764.9	0.949
z3	2.9	40	6.1	1098.7	0.326	0.126249	(.20)	1.1286	(.29)	0.06483	(.20)	766.4	767.1	768.9	0.725
BVL-0057															
z1	0.4	975	123.2	737.0	0.241	0.111029	(1.12)	0.9879	(1.15)	0.06453	(.23)	678.7	697.7	759.1	0.979
z2	0.5	278	32.5	380.7	0.269	0.101809	(.54)	0.9052	(.65)	0.06449	(.34)	625.0	654.5	757.7	0.856

(a) Measured ratio corrected for spike and fractionation only. (b) Radiogenic Pb. (c) Corrected for fractionation, spike, blank, and initial common Pb. (d) All uncertainties are given as 2σ errors in %.Mass fractionation correction of $0.15\text{‰}/\text{amu} \pm 0.04\text{‰}/\text{amu}$ (atomic mass unit) was applied to single-collector Daly analyses and $0.12\text{‰}/\text{amu} \pm 0.04\text{‰}$ for dynamic Faraday–Daly analyses.

Total procedural blank was less than 1.0 pg for U.

Blank isotopic composition: $^{206}\text{Pb}/^{204}\text{Pb} = 19.10 \pm 0.1$; $^{207}\text{Pb}/^{204}\text{Pb} = 15.71 \pm 0.1$; $^{208}\text{Pb}/^{204}\text{Pb} = 38.65 \pm 0.1$.

Corr. coef. = correlation coefficient.

Age calculations are based on the decay constants of Steiger and Jäger (1977).

Common-Pb corrections were calculated by using the model of Stacey and Kramers (1975) and the interpreted age of the sample.

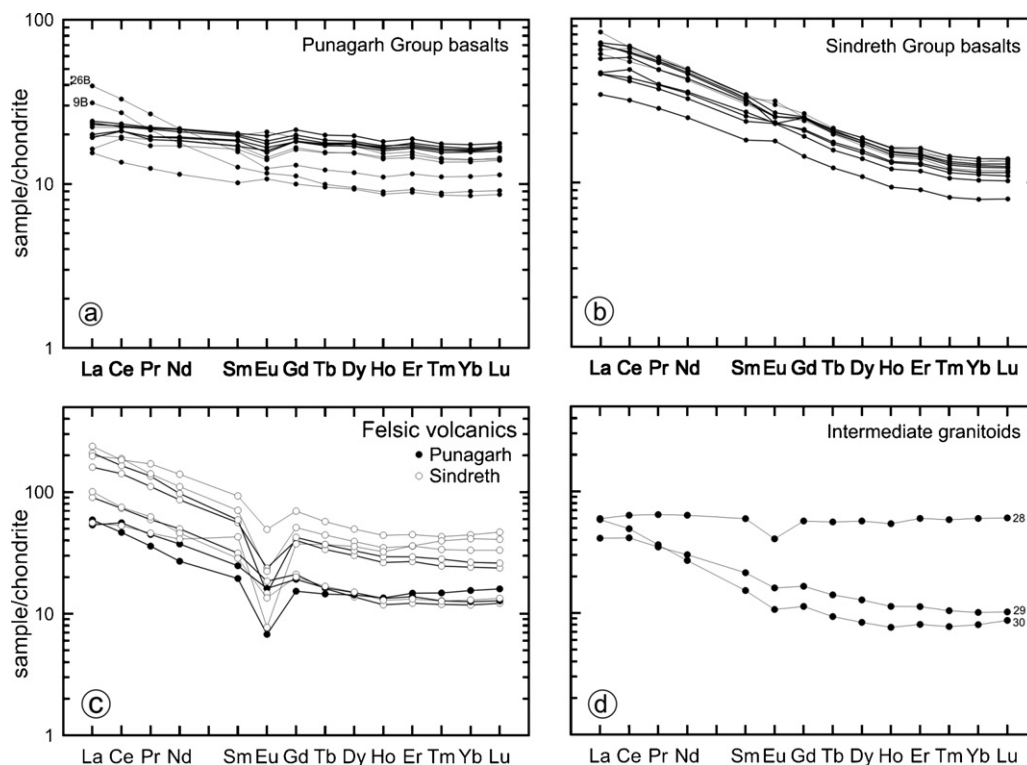


Fig. 9. Chondrite-normalized REE plots for (a) Punagarh Group basalts, (b) Sindreth Group basalts, (c) Punagarh and Sindreth felsic volcanics and (d) intermediate granitoids. Chondrite abundances are from [Anders and Grevesse \(1989\)](#).

chlorite has caused the release of Ca, which was partially reprecipitated as calcite, epidote and sphene ([Table 1](#)). In many cases there appears to have been absolute loss of Ca, with or without accompanying gain of Na, as shown by the decline of $\text{CaO}/\text{Na}_2\text{O}$ with increasing values of LOI ([Fig. 8a](#)). This is obviously reflected mineralogically, as those samples preserving primary mineralogy to the highest degrees have the highest $\text{CaO}/\text{Na}_2\text{O}$ and lowest LOI values ([Table 2](#)).

Other chemical effects associated with hydrothermal alteration in the Punagarh and Sindreth mafic rocks include U mobility, which is especially evident in Punagarh basalts. This is illustrated on a Nb/Th vs. Nb/U diagram in [Fig. 8b](#). Many of the samples plot along a “magmatic array”, representing a mixing trend between the compositions of a mantle source and that of continental crust. Other samples, however, are displaced from this array, mainly to higher, and to a lesser extent, lower Nb/U. Punagarh basalts, for example, are displaced to higher Nb/U at relatively constant Nb/Th, which is an indicator of U-loss associated with secondary alteration. A few of the Sindreth basalts are displaced toward lower Nb/U, indicative of U-gain. Mobility of U has been documented in hydrothermal alteration of modern oceanic basalts, whereas Th, Nb, Ti, REE and Zr are generally immobile (e.g. [Staudigel, 2003](#)). In the Punagarh and Sindreth mafic rocks, these insoluble, immobile elements show no obvious correlations with chemical indicators of secondary processes, and we propose that their concentrations have remained primary, or nearly so. Some, but not all of these effects have been observed in studies of spilitic rocks (e.g. [Cann, 1969](#); [Hellman and Henderson, 1977](#); [Levi et al., 1982](#); [Sethna and Javeri, 1999](#); [Vallance, 1974](#)). In general the Sindreth mafic rocks show a higher degree of alteration effects, although there is considerable overlap, for example in LOI content.

We propose that the low-grade alteration features present in the Punagarh and Sindreth basaltic rocks formed as a result of hydrothermal processes associated with basalt-seawater interactions in newly formed oceanic crust. Although we cannot at this

time rule out simple burial metamorphism, for example during a younger basin-forming event, the superbly preserved magmatic textures and structures in Punagarh and Sindreth basalts argue against any type of regional metamorphism that was accompanied by deformation. Dating of alteration minerals, for example using the Ar–Ar isotopic system on amphibole, might distinguish syn-magmatic ocean-floor metamorphism from a younger burial metamorphism, but this is beyond the scope of our study.

6.2. Pre-alteration chemical and petrological features

Which features of the Punagarh and Sindreth igneous rocks are primary? This is difficult to constrain, given their variable, but generally high degree of hydrothermal alteration. We do consider the dominantly olivine tholeiitic normative compositions for the mafic rocks, and the intermediate nature of the dacites and rhyolites as largely original. Likewise, the differences in overall REE patterns between the Punagarh and Sindreth basalts appear to be primary, given the lack of correlation between LOI and REE concentrations or pattern shapes. In general, Sindreth basalts have slightly higher REE abundances and steeper LREE-enriched patterns relative to Punagarh basalts, for which pattern shapes are quite flat ([Fig. 9](#)). Two Punagarh basalt samples, however (BVL-9B and BVL-26B), have REE patterns more akin to Sindreth basalts ([Fig. 9a and b](#)). The overall differences in REE pattern shapes for basalts from the two Groups may be attributable to slightly larger degrees of partial melting of a putative mantle source for the Punagarh samples relative to Sindreth ones. This would be consistent with the higher Mg# values of Punagarh basalts ($\text{Mg\#} = 0.38\text{--}0.62$, avg. = 0.47, $n = 12$) relative to Sindreth basalts ($\text{Mg\#} = 0.17\text{--}0.50$, avg. = 0.39, $n = 10$) ([Table 2](#)), although there is considerable overlap, and we consider this conclusion tentative. The small negative Eu anomalies in many of the basalts from both Groups can be explained by 3–5% plagioclase fractionation.

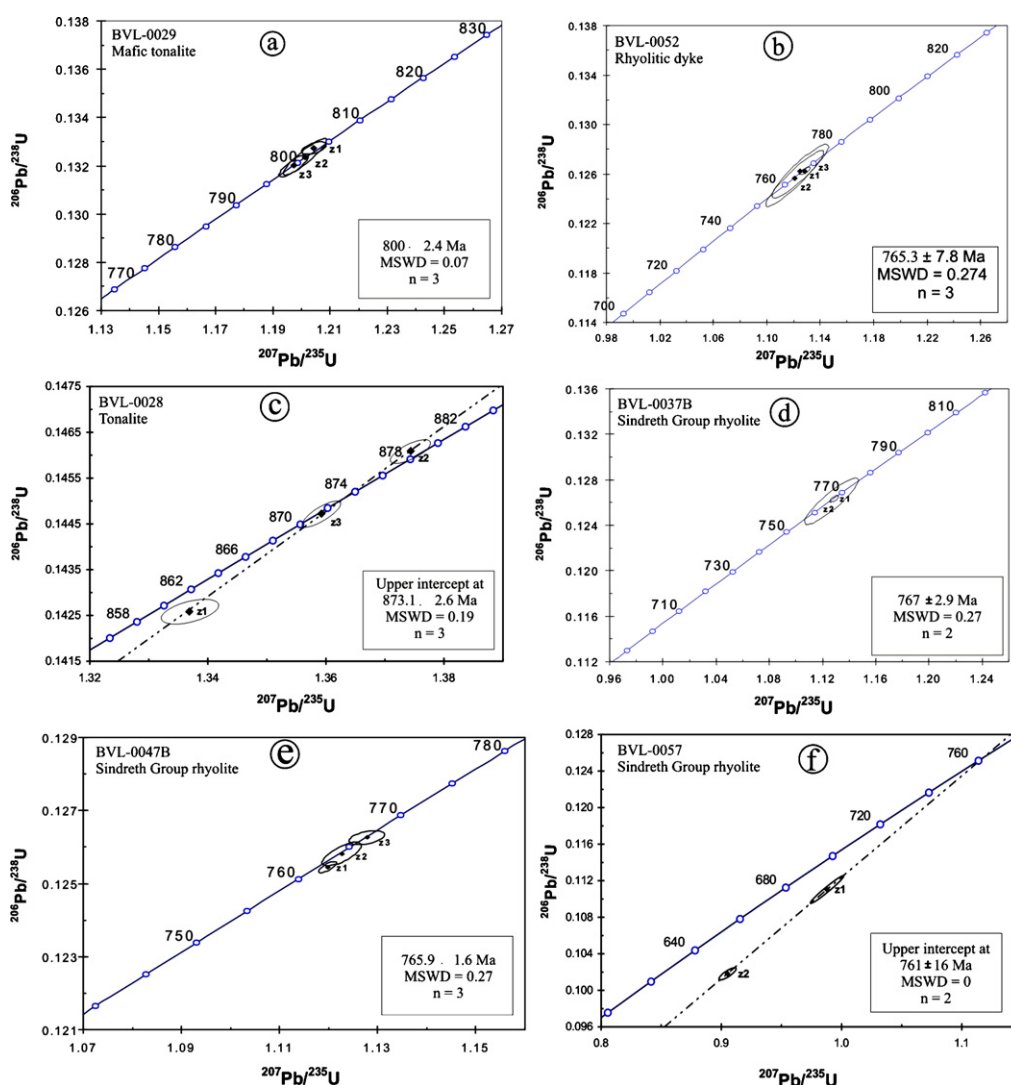


Fig. 10. Concordia diagrams showing U–Pb zircon analyses for individual rocks: (a) mafic tonalite BVL-0029, (b) rhyolitic dyke BVL-0052, (c) tonalite BVL-0028, (d) rhyolite BVL-0037B, (e) rhyolite BVL-0047B and (f) rhyolite BVL-0057. Analytical uncertainties shown are at 2σ confidence levels. Ages indicated in the insets are weighted mean $^{207}\text{Pb}/^{206}\text{Pb}$ ages.

An intriguing array is apparent on the Nb/Th vs. Nb/U diagram (labelled “magmatic array” in Fig. 8b). Similar arrays have been interpreted, for example, as representing mixing between a mantle component with high Nb/U, and a continental crustal component with low Nb/U (Sylvester et al., 1997). The mantle component in the Punagarh/Sindreh array has Nb/U ~ 50, implying depletion of U relative to Nb due to continental crust formation, and is similar to the mean Nb/U of modern MORBs and OIBs (e.g. Hofmann, 2003).

The Punagarh mafic rocks all have positive $\varepsilon_{\text{Nd},750}$ values (+1.64 to +5.18), indicating derivation from a mantle source with long-term depletion in LREE. Although there is some overlap, Sindreh mafic rocks have lower $\varepsilon_{\text{Nd},750}$ values (–2.11 to +3.56), which probably indicates contamination with an ancient continental crustal component. If so, this component could be represented in material such as the nearby Archaean Banded Gneiss Complex (BGC, Fig. 1), but we cannot rule out that at least some of the reduction in $\varepsilon_{\text{Nd},750}$ values was caused by secondary processes such as hydrothermal alteration.

6.3. Implications from U–Pb geochronology

The age of the Sindreh Group felsic volcanic rocks is directly dated in this study by U–Pb zircon methods, which yield

767 ± 2.9 Ma (dacite, BVL-0037B), 765.9 ± 1.6 Ma (rhyolite, BVL-0047B) and 761 ± 16 Ma (rhyolite, BVL-0057). By inference, we propose that the interlayered mafic volcanic rocks are coeval, representing a period of bimodal mafic and felsic volcanism at about 765 Ma. By contrast, we were unable to provide direct constraints on the age of volcanism in the Punagarh Group, because zircon-bearing felsic rocks are not obviously exposed there. However, the Punagarh volcanics must be younger than 800 ± 2.4 Ma, the age of mafic tonalite BVL-0029, which represents the basement upon which the Punagarh lavas were erupted. Our data are therefore consistent with eruption of the Sindreh and Punagarh volcanics at about the same time; such coevality is supported by their geological, petrological and geochemical similarities. Also coeval with this volcanism is the 765.3 ± 7.8 Ma rhyolite porphyry dike (BVL-0052) that crosscuts phyllites of the Delhi Supergroup about 25 km south of the Sindreh Belt (Fig. 1). We note with great interest that the ages of these rocks are within error of U–Pb zircon results for the widespread and voluminous Malani rhyolites (751–771 Ma, Torsvik et al., 2001a; Gregory et al., 2009). A connection between Punagarh, Sindreh and Malani volcanism had been suggested on geological grounds by Roy and Sharma (1999).

A secondary result of our geochronology relates to the time span of magmatism historically referred to as “Erinapura” granites. Previ-

Table 4
Sm and Nd isotopic compositions for Punagarh and Sindreth rocks.

Locality and sample no.	Rock type	Sm (ppm)	Nd (ppm)	$^{147}\text{Sm}/^{144}\text{Nd}$	Uncertainty	$^{143}\text{Nd}/^{144}\text{Nd}$	Uncertainty	Epsilon today ^a	Epsilon 765 Ma ^a	T(DM) Ma ^b	U–Pb zircon age (Ma)
Punagarh Group											
BVL-005B	Dacite	7.97 ± 0.022	36.71 ± 0.09	0.13124	0.00056	0.512358	0.000004	−5.47 ± 0.07	0.94	1264	
BVL-005C	Basalt	5.60 ± 0.015	18.64 ± 0.05	0.18161	0.00078	0.512653	0.000006	0.29 ± 0.12	1.77	1838	
BVL-005C(2)	Basalt	5.35 ± 0.014	17.72 ± 0.04	0.18258	0.00077	0.512651	0.000004	0.25 ± 0.07	1.64	1906	
BVL-008B	Basalt	5.79 ± 0.015	19.66 ± 0.05	0.17813	0.00078	0.512686	0.000023	0.93 ± 0.45	2.76	1515	
BVL-008B(2)	Basalt	5.62 ± 0.015	19.07 ± 0.05	0.17831	0.00076	0.512626	0.000004	−0.23 ± 0.07	1.57	1780	
BVL-0016(2)	Dolerite	3.80 ± 0.010	13.10 ± 0.03	0.17540	0.00075	0.512793	0.000004	3.02 ± 0.07	5.12	1001	
BVL-0019(2)	Basalt	5.34 ± 0.014	18.59 ± 0.05	0.17360	0.00074	0.512759	0.000003	2.35 ± 0.06	4.63	1082	
BVL-0020	Dolerite/Gabbro	6.00 ± 0.016	21.21 ± 0.05	0.17099	0.00074	0.512774	0.000004	2.66 ± 0.07	5.18	967	
BVL-0029(2)	Diorite/Tonalite	6.59 ± 0.017	29.70 ± 0.07	0.13414	0.00057	0.512308	0.000003	−6.44 ± 0.06	−0.32	1404	
BVL-0030	Granite	4.99 ± 0.013	28.13 ± 0.07	0.10716	0.00046	0.512172	0.000004	−9.08 ± 0.07	−0.33	1244	
Sindreth Group											
BVL-0037A	Basalt	24.02 ± 0.062	106.41 ± 0.26	0.13649	0.00058	0.512431	0.000003	−4.04 ± 0.05	1.86	1207	
BVL-0038	Basalt	4.89 ± 0.013	21.32 ± 0.05	0.13866	0.00059	0.512529	0.000004	−2.13 ± 0.07	3.56	1047	
BVL-0046C	Basalt	8.78 ± 0.023	38.84 ± 0.10	0.13665	0.00058	0.512377	0.000003	−5.09 ± 0.06	.79	1314	
BVL-0047A	Dolerite	7.77 ± 0.021	35.28 ± 0.09	0.13313	0.00057	0.512450	0.000003	−3.67 ± 0.06	2.56	1123	
BVL-0049	Basalt	12.98 ± 0.292	50.97 ± 0.13	0.15402	0.00412	0.512316	0.000004	−6.29 ± 0.07	−2.11	1851	
BVL-0057	Rhyolite	11.74 ± 0.030	35.58 ± 0.09	0.19957	0.00084	0.512554	0.000004	−1.64 ± 0.07	−1.92		761 ± 18/−14

^a Using CHUR parameters $^{147}\text{Sm}/^{144}\text{Nd} = 0.1967$, $^{143}\text{Nd}/^{144}\text{Nd} = 0.512638$.

^b Using depleted mantle model of DePaolo et al. (1991).

ous results based on Rb–Sr (815 ± 30 Ma, Choudhary et al., 1984) and U–Pb ($836 \pm 7/-5$ Ma, Deb et al., 2001) implied a relatively restricted time period for intrusion of these granitoids. Our data extend this range from 800 ± 2.4 Ma (mafic tonalite BVL-0029) to 873.1 ± 2.6 Ma (tonalite BVL-0028). Further work will be needed to constrain the timing and tectonic significance of this magmatism, but in any case our results imply that “Erinapura-type” granitoid magmatism is distinctly older than, and unrelated to the Punagarh, Sindreth and Malani igneous activity. Finally, the supracrustal rocks of the Delhi Supergroup, which are crosscut by Erinapura granites, must be older than about 870 Ma, at least in the region of the Aravalli Craton covered by our sampling.

6.4. Tectonic setting and late precambrian evolution of the Aravalli Craton

Any model for the tectonic setting of the volcanic and associated rocks of the Punagarh and Sindreth basins must take into account the following features: the presence of dominantly bimodal basaltic and rhyolitic lavas, with abundant pillow structures in the mafic rocks, pervasive splilitic-type hydrothermal alteration, clastic sedimentary rocks interlayered with the lavas, and unconformable relationships of the volcanic rocks upon dominantly clastic metasedimentary rocks of the Delhi Supergroup. There is also the evidence from Nd isotopes for derivation from depleted mantle, with variable contamination by old continental crust, especially for Sindreth samples, which have $\epsilon_{\text{Nd},750}$ values as low as -2.11 . These features effectively eliminate a mid-ocean ridge setting; remaining possibilities include continental rift, plume and back-arc settings.

It is difficult to distinguish conclusively between these possibilities, given the incomplete preservation and exposure of these Neoproterozoic rocks. The presence of hydrothermally altered basaltic pillow lavas in the Punagarh and Sindreth basins tends to argue against continental rift or plume settings, as such rocks are not abundant in those environments. We note with interest that approximately coeval mafic igneous rocks with similar low-grade mineral compositions occur in the Gariep Orogen of SW Namibia. These include a dike swarm of variably metamorphosed dolerites (Gannakouriep Suite) and dominantly felsic with minor mafic volcanic rocks (Rosh Pinah Formation). These magmatic rocks, however, are best interpreted as having formed during continental rifting (Frimmel, 2008). For the Punagarh and Sindreth Groups, we favour a back-arc basin setting, which we feel is most consistent with the observed features. A relevant analogy from younger rocks might include the Cretaceous back-arc basin of South Georgia (Scotia Arc). Here, rocks of the back-arc basin system consist of massive, amygdaloidal and pillowed basaltic lavas, lava breccias, dacites, rhyolites, tuffs and basic dykes (Storey and Mair, 1982). The basaltic pillow lavas contain mineralogical features typical of oceanic hydrothermal systems, including albitized microphenocrysts, altered, formerly glassy groundmass, mafic mineral assemblages varying between prehnite–pumpellyite and lower amphibolite facies, with well preserved primary clinopyroxene. Interlayered sedimentary rocks include continent-derived silicic volcanoclastics, laminated mudstones and massive immature sandstones. These features are sufficiently similar to those present in the Punagarh and Sindreth basins to consider a direct analogy with Mesozoic and younger back-arc basins (c.f. Bruhn et al., 1978; De Wit and Stern, 1981; Stern, 1991).

If a back-arc basin model for the Punagarh and Sindreth volcanic rocks can be seriously entertained, then this calls into question their relationships with the nearby felsic magmatic rocks of the Malani Igneous Suite, which have conventionally been interpreted as having formed in a continental rift or hotspot-related environment (e.g. Pareek, 1981; Bhushan, 1995). Indeed, palaeomagnetic data

for 750–770 Ma Malani felsic volcanics (Torsvik et al., 2001a) and 750 Ma dolerites and coeval granitoids of the Seychelles (Torsvik et al., 2001b) place these regions, along with the Neoproterozoic magmatic rocks of west-central Madagascar (Handke et al., 1999), together in a continental margin position along the western edge of the Rodinia supercontinent. These and other authors (e.g. Ashwal et al., 2002) have interpreted all of these magmatic rocks as having formed in an Andean-type continental arc environment.

Acknowledgements

This study was done in partial fulfillment for the M.Sc degree of the senior author at Rand Afrikaans University, South Africa, under the supervision of Profs. L.D. Ashwal, M.K. Pandit and S.A. Bowring. Funds were supplied by research grants to Prof. T.H. Torsvik (Norwegian Research Council) and Prof. L.D. Ashwal (National Research Foundation, South Africa). We gratefully acknowledge support from the Department of Science and Technology (New Delhi) and National Research Foundation (Pretoria) under the Indo-South African Inter-Governmental Science & Technology Co-operation Programme. The authors are indebted to Frank Dudas and Jahan Ramezani for assistance with Sm–Nd isotope and U–Pb zircon analyses (MIT). Prof. Anton le Roex and Fran Pocock (Univ. of Cape Town) are thanked for their assistance in obtaining ICP-MS and XRF data. We thank Dr. K.K. Sharma, Pankaj Saini and Shailendra Singh for valuable discussions and/or fieldwork at Sindreh. Paul Sylvester helped us with some geochemical aspects of alteration processes. Comments by Pat Bickford and an anonymous reviewer are gratefully appreciated.

References

- Ahmad, T., Tarney, J., 1994. Geochemistry and petrogenesis of late Archaean Aravalli volcanics, basement enclaves and granitoids, Rajasthan. *Precam. Res.* 65, 1–23.
- Anders, E., Grevesse, N., 1989. Abundances of the elements: meteoric and solar. *Geochim. Cosmochim. Acta* 53, 197–214.
- Ashwal, L.D., Demaiffe, D., Torsvik, T.H., 2002. Petrogenesis of Neoproterozoic granitoids and related rocks from the Seychelles: the case for an Andean-type arc origin. *J. Petrol.* 43, 45–83.
- Bhushan, S.K., 1995. Late Proterozoic continental growth: implications from geochemistry of acid magmatic events of West Indian Craton, Rajasthan. *Mem. Geol. Soc. India* 34, 339–355.
- Bhushan, S.K., 2000. Malani rhyolites—a review. *Gondwana Res.* 3, 65–77.
- Biju Sekhar, S., Yokoyama, K., Pandit, M.K., Okudaira, T., Santosh, M., 2003. Paleoproterozoic magmatism in Delhi Fold Belt, NW Indian and its significance: evidence from EPMA chemical ages of zircons. *J. Asian Earth Sci.* 22, 189–207.
- Bose, U., 1989. Correlation problems of the Proterozoic stratigraphy of Rajasthan. *Indian Miner.* 43, 183–193.
- Bruhn, R.L., Stern, C.R., De Wit, M.J., 1978. Field and geochemical data bearing on the development of a Mesozoic volcano-tectonic rift zone and back-arc basin in southernmost South America. *Earth Planet. Sci. Lett.* 41, 32–46.
- Cann, J.R., 1969. Spilites from the Carlsberg Ridge. *Indian Ocean. J. Petrol.* 10, 1–19.
- Chore, S.A., 1990. Precambrian stratigraphy of Western Rajasthan in parts of Pali and Sirohi districts. *Rec. Geol. Surv. India* 123, 9.
- Chore, S.A., Mohanty, M., 1998. Stratigraphic and tectonic setting of the Trans-Aravalli Neoproterozoic volcanosedimentary sequences in Rajasthan. *J. Geol. Soc. India* 51, 57–68.
- Choudhary, A.K., Gopalan, K., Sastry, C.A., 1984. Present status of the geochronology of the Precambrian rocks of Rajasthan. *Tectonophysics* 105, 131–140.
- Crawford, A.R., Compston, W., 1970. The age of the Vindhyan System of Peninsular India. *Q. J. Geol. Soc. London* 125, 351–371.
- Deb, M., Thorpe, R.L., Krstic, D., Corfu, F., Davis, D.W., 2001. Zircon U–Pb and galena Pb isotope evidence for an approximate 1.0 Ga terrane constituting the western margin of the Aravalli–Delhi orogenic belt, northwestern India. *Precam. Res.* 108, 195–213.
- DePaolo, D.J., Linn, A.M., Schubert, G., 1991. The continental crustal age distribution: methods of determining mantle separation ages from Sm–Nd isotopic data and applications to the southwestern United States. *J. Geophys. Res.* 96, 2071–2088.
- De Wit, M.J., Stern, C.R., 1981. Variations in the degree of crustal extension during formation of a back-arc basin. *Tectonophysics* 72, 229–260.
- Dhar, S., Frei, R., Kramers, J.D., Nägler, T.F., Kochhar, N., 1996. Sr, Pb and Nd isotope studies and their bearing on the petrogenesis of the Jalor and Siwana complexes, Rajasthan, India. *J. Geol. Soc. India* 48, 151–160.
- Duncan, A.R., Erlank, A.J., Betton, P.J., 1984. Analytical techniques and database descriptions. *Spec. Publ. Geol. Soc. S. Afr.*, 13, Appendix 1, 389–395.
- Eby, G.N., Kochhar, N., 1990. Geochemistry and petrogenesis of the Malani igneous suite, Northern India. *J. Geol. Soc. India* 36, 109–130.
- Frimmel, H.E., 2008. Neoproterozoic Gariep Orogen. In: Miller, R.McG. (Ed.), *The Geology of Namibia*, Vol. 2, Neoproterozoic to Lower Proterozoic. Geological Survey of Namibia, Windhoek, pp. 14–1–14–39.
- Gopalan, K., Macdougall, J.D., Roy, A.B., Murali, A.V., 1990. Sm–Nd evidence for 3.3 Ga old rocks in Rajasthan, northern India. *Precam. Res.* 48, 287–297.
- Gregory, L.C., Meert, J.G., Bingen, B., Pandit, M.K., Torsvik, T.H., 2009. Paleomagnetism and geochronology of Malani Igneous Suite, northwest India: implications for the configuration of Rodinia and assembly of Gondwana. *Precam. Res.* 170, 13–26.
- Gupta, S.N., Arora, Y.K., Mathur, R.K., Iqbaluddin, Prasad, B., Sahai, T.N., Sharma, S.B., 1997. The Precambrian geology of the Aravalli region, southern Rajasthan and north-eastern Gujarat, India (with geological map, Scale 1:250,000). *Mem. Geol. Surv. India* 123, 262 pp.
- Handke, M.J., Tucker, R.D., Ashwal, L.D., 1999. Neoproterozoic continental arc magmatism in west-central Madagascar. *Geology* 27, 351–354.
- Heinrich, K.F.J., 1986. Mass absorption coefficients for electron probe microanalysis. In: Brown, J.B., Packwood, R.H. (Eds.), *Proc. 11th Int. Congress on X-ray Optics and Microanalysis*. London, Canada.
- Hellman, P.L., Henderson, P., 1977. Are rare earth elements mobile during spilitization? *Nature* 267, 38–40.
- Heron, A.M., 1953. *Geology of Central Rajputana*. Mem. Geol. Surv. India 79, 389 pp.
- Hofmann, A.W., 2003. Sampling Mantle Heterogeneity through Oceanic Basalts: Isotopes and Trace Elements. *Treatise on Geochemistry*. Elsevier, Amsterdam, chapter 2.03m 61–101.
- Levi, B., Aguirre, L., Nyström, J.O., 1982. Metamorphic gradients in burial metamorphosed vesicular lavas: comparison of basalt and spilitite in Cretaceous basic flows from central Chile. *Contrib. Mineral. Petrol.* 80, 49–58.
- Mukherjee, A., 1966. Tectonics of Late Precambrian ignimbrites in western Rajasthan (India)—discussion. *Geologie en Mijnbouw* 45, 193–196.
- Naha, K., Halyburton, R.V., 1974. Early Precambrian stratigraphy of central and southern Rajasthan, India. *Precam. Res.* 1, 55–73.
- Naha, K., Roy, A.B., 1983. The problem of Precambrian basement in Rajasthan, Western India. *Precam. Res.* 19, 217–223.
- Norrish, K., Hutton, J.T., 1969. An accurate X-ray spectrographic method for the analysis of a wide range of geological samples. *Geochim. Cosmochim. Acta* 33, 431–453.
- Pandit, M.K., Carter, L.M., Ashwal, L.D., Tucker, R.D., Torsvik, T.H., Jamtveit, B., Bhushan, S.K., 2003. Age, petrogenesis and significance of Early Neoproterozoic granitoids and related rocks from the Sendra area, Aravalli Craton, NW India. *J. Asian Earth Sci.* 22, 363–381.
- Pandit, M.K., Sial, A.N., Jamrani, S.S., Ferreira, V.P., 2001. Carbon isotopic profile across the Bilara Group rocks of Trans-Aravalli Marwar Supergroup in western India: implications for Neoproterozoic–Cambrian transition. *Gondwana Res.* 4, 387–394.
- Pareek, H.S., 1981. Petrochemistry and petrogenesis of the Malani Igneous Suite, India. *Geol. Soc. Am. Bull.* 92, 206–273.
- Rathore, S.S., Venkatesan, T.R., Srivastava, R.K., 1996. Mundwara alkali igneous complex, Rajasthan, India; chronology and Sr isotope systematics. *J. Geol. Soc. India* 48, 517–528.
- Rathore, S.S., Venkatesh, T.R., Srivastava, R.K., 1999. Rb–Sr isotope dating of Neoproterozoic (Malani Group) magmatism from South-west Rajasthan, India: evidence of younger Pan-African thermal event by ^{40}Ar – ^{39}Ar studies. *Gondwana Res.* 2, 271–286.
- Roy, A.B., Jakhar, S.R., 2002. *Geology of Rajasthan (Northwest India)—Precambrian to Recent*. Scientific Publishers (India), Jodhpur, 421 pp.
- Roy, A.B., Kröner, A., 1996. Single zircon evaporation ages constraining the growth of the Archaean Aravalli craton, northwestern Indian shield. *Geol. Mag.* 133, 333–342.
- Roy, A.B., Sharma, K.K., 1999. Geology of the region around Sirohi Town, Western Rajasthan—Story of Neoproterozoic evolution of the Trans-Aravalli crust. In: Paliwal, B.S. (Ed.), *Geological Evolution of NW Indian Crust*. Scientific Publishers (India), Jodhpur, pp. 19–33.
- Saini, P., Singh, S., Pandit, M.K., 2006. Angular relationship between rocks of Aravalli and Delhi Supergroups in southeastern Rajasthan. *Curr. Sci.* 91, 432–434.
- Sethna, S.F., Javeri, P., 1999. Geology and petrochemistry of the Deccan spilitic basalts at and around Daman, India. *J. Geol. Soc. India* 53, 59–69.
- Sharma, R.S., 1977. Deformational and crystallisation history of the Precambrian rocks in north-central Aravalli Mountain, Rajasthan, India. *Precam. Res.* 4, 133–162.
- Sharma, R.S., 1995. An evolutionary model for the Precambrian crust of Rajasthan: some petrological and geochronological considerations. *Mem. Geol. Soc. India* 31, 91–115.
- Singh, S.P., 1982. Pillow lavas from Delhi Supergroup near Bambholai, Pali District, Rajasthan. *J. Geol. Soc. India* 24, 208–211.
- Sinha-Roy, S., 1984. Precambrian crustal interaction in Rajasthan, NW India. In: *Proc. Seminar on crustal evolution of Indian Shield*. Proc. and its bearings on Metallogeny. Indian J. Earth Sci., pp. 84–91.
- Sinha-Roy, S., Malhotra, G., Mohanty, M., 1998. *Geology of Rajasthan*. Geol. Soc. India, Bangalore, India, 278 pp.
- Sivaraman, T.V., Raval, U., 1995. U–Pb isotopic study of zircons from a few granitoids of Delhi–Aravalli Belt. *J. Geol. Soc. India* 46, 164–475.
- Stacey, J.S., Kramers, J.D., 1975. Approximation of terrestrial lead isotope evolution by a two-stage model. *Earth Planet. Sci. Lett.* 26, 207–221.

- Staudigel, H., 2003. Hydrothermal Alteration Processes in the Oceanic Crust. *Treatise on Geochemistry*. Elsevier, Amsterdam, Chapter 3.15, 511–535.
- Steiger, R.H., Jäger, E., 1977. Subcommittee on geochronology: convention on the use of decay constants in geo- and cosmochronology. *Earth Planet. Sci. Lett.* 36, 359–362.
- Stern, C.R., 1991. Isotopic composition of Late Jurassic and Early Cretaceous mafic igneous rocks from the southernmost Andes: implications for sub-Andean mantle. *Rev. Geol. Chile* 18, 15–23.
- Storey, B.C., Mair, B.F., 1982. The composite floor of the Cretaceous back-arc basin of South Georgia. *J. Geol. Soc. London* 139, 729–737.
- Sugden, T.J., Deb, M., Windley, B.F., 1990. Tectonic setting of mineralization in the Proterozoic Aravalli-Delhi orogenic belt, NW India. In: Naqvi, S.M. (Ed.), *Precambrian Continental Crust and its Economic Resources*. Developments in Precambrian Geology, vol. 8. Elsevier, Amsterdam, pp. 367–390.
- Sun, S.-S., 1982. Chemical composition and origin of the Earth's primitive mantle. *Geochim. Cosmochim. Acta* 46, 179–192.
- Sylvester, P.J., Campbell, I.H., Bowyer, D.A., 1997. Niobium/Uranium evidence for early formation of the continental crust. *Science* 275, 521–523.
- Torsvik, T.H., Carter, L.M., Ashwal, L.D., Bhushan, S.K., Pandit, M.K., Jamtveit, B., 2001a. Rodinia refined or obscured: Palaeomagnetism of the Malani Igneous Suite (NW India). *Precam. Res.* 108, 319–333.
- Torsvik, T.H., Ashwal, L.D., Tucker, R.D., Eide, E.A., 2001b. Neoproterozoic geochronology and palaeogeography of the Seychelles microcontinent: the India link. *Precam. Res.* 110, 47–59.
- Vallance, T.G., 1974. Spilitic degradation of a tholeiitic basalt. *J. Petrol.* 15, 79–96.
- Volpe, A.M., Macdougall, J.D., 1990. Geochemistry and isotopic characteristics of mafic (Phulad Ophiolite) and related rocks in the Delhi Supergroup, Rajasthan, India: implications for rifting in the Proterozoic. *Precam. Res.* 48, 167–191.
- Wiedenbeck, M., Goswami, J.N., 1994. An ion-probe single zircon $^{207}\text{Pb}/^{206}\text{Pb}$ age from the Mewar Gneiss at Jhamarkotra, Rajasthan. *Geochim. Cosmochim. Acta* 58, 2135–2141.
- Wiedenbeck, M., Goswami, J.N., Roy, A.B., 1996. Stabilisation of the Aravalli Craton of northwestern India at 2.5 Ga: an ion microprobe zircon study. *Chem. Geol.* 129, 325–340.